FUNDAMENTALS OF OPTICAL FIBER TRANSMISSION

Technical University of Lodz, Laboratory of Laser Molecular Spectroscopy, 93- 590 Lodz, Wroblewskiego 15 str, Poland, abramczy@mitr.p.lodz.pl,
www.mitr.p.lodz.pl/raman
, www.mitr.p.lodz.pl/evu
Max Born Institute, Marie Curie Chair, 12489 Berlin, Max Born Str 2A,
abramczy@mbi-berlin.de

1.1. Introduction – Physical Fundamentals of Optical Fiber Transmission
1.2. Snell's Law and Critical Angle for Total Internal Reflection
1.3. Optical Fiber Types
1.4. Propagation of Light in Optical Fibers. Electrodynamic Analysis.
1.4.1. Step-Index Cylindrical Fiber
1.4.2. TE (Or H) Modes
1.4.3. TH (Or E) Modes
1.4.4. Hybrid Modes EH and HE
1.4.5. TE_{mp}, TM_{mp}, HE_{mp}, EH_{mp} Modes
1.4.6. Cut-Off Frequency
1.4.7. Linear Polarization Modes Lp_{mp}
1.5. Propagation of Light in Optical Fibers. Electrodynamic Analysis. Planar Optical Waveguide. Graphical Solution of Characteristic Equation.
1.6. Propagation of Light in Optical Fibers. Analysis of Optical Path and Electrodynamic Analysis for Gradient-Index Cylindrical Fiber
1.7. Optical Glass Fiber Production
1.8. Optical Windows for transmission
1.9. Generations of Optical Fiber Transmission

1.1. Introduction – Physical Fundamentals of Optical Fiber Transmission

Light is used in optoelectronics and optical fiber telecommunication for data transmission, in optical fiber interferometers, optical fiber lasers, sensors and optical fiber modulators. The term "light" in fiber transmission, even though commonly used, is not always precise: Light defines only the electro-magnetic radiation from the visual range of 380-780 nm, while in many applications, e.g. optical fiber transmission, the electro-magnetic radiation from near infrared range (850 nm, 1310 nm, 1550 nm) is used. Fig. 1.1. shows the electromagnetic radiation spectrum and allows to locate the radiation used in optical fiber transmission. In further parts of this book the terms "light" and "electro-magnetic radiation from near infrared range" will be used interchangeably.

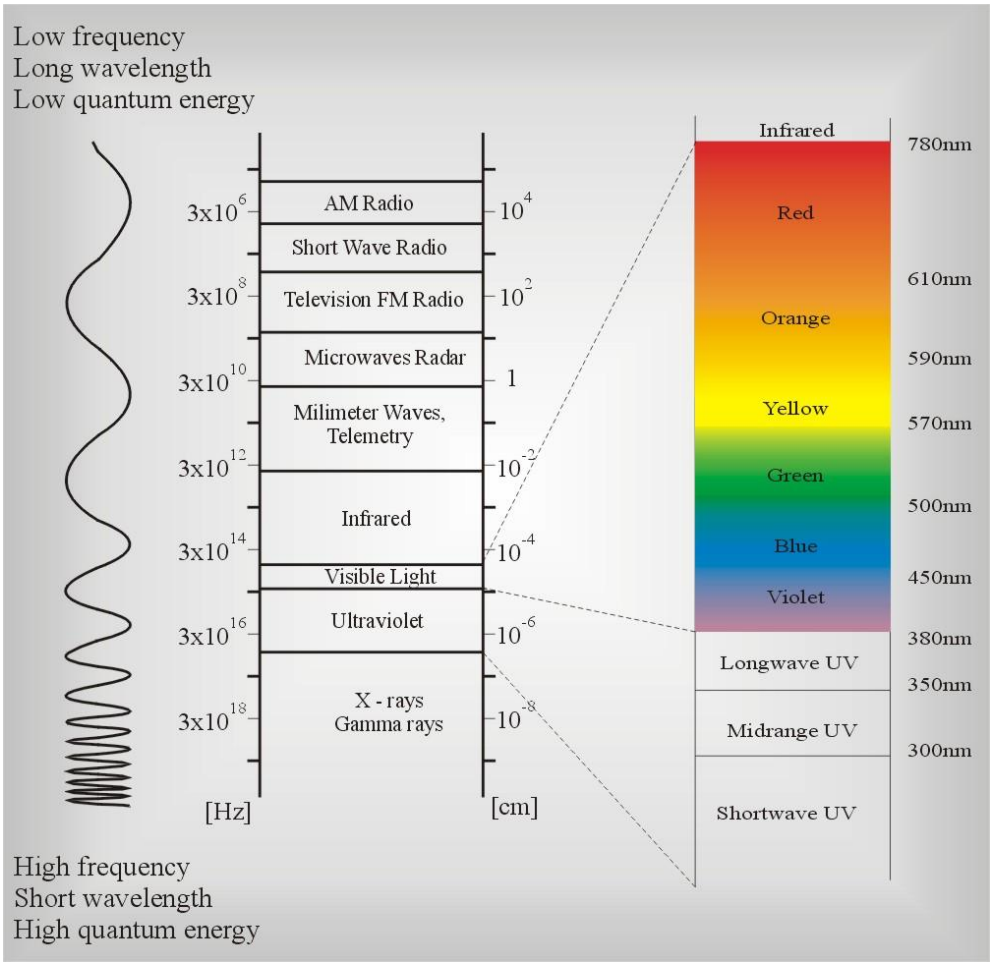

Fig. 1.1. Electromagnetic radiation spectrum

The optical fiber is a waveguide used for transmission of light. It consists of a dielectric fiber core, usually from glass, surrounded by a layer of glass or plastic cladding characterized by the refraction index lower than that of the core. The light transmitted through the optical fiber is trapped inside the core due to the total internal reflection phenomenon. The total internal reflection occurs at the core-cladding interface when the light inside the core of the fiber is incident at an angle greater than the critical angle Θ_{cr} and returns to the core lossless and allows for light propagation along the fiber. The amount of light reflected at the interface changes depending on the incidence angle and the refraction indexes of the core and the cladding. Fig. 1.2. presents the idea of the light propagation in the cylindrical optical fiber due to the total internal reflection.

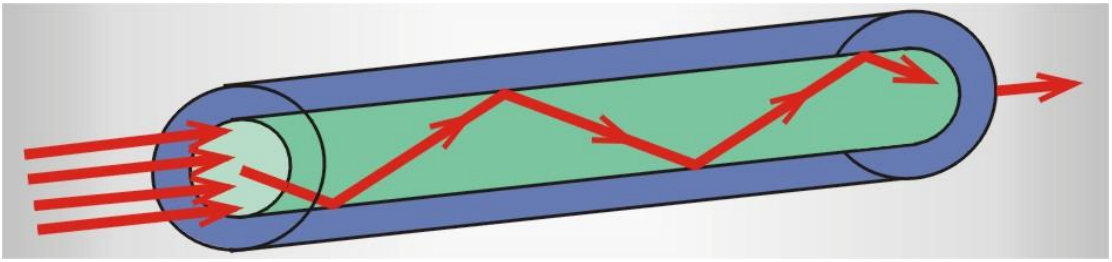

Fig. 1.2. Diagram of cylindrical optical fiber.

1.2. Snell's Law and Critical Angle for Total Internal Reflection

Let us recollect the idea of the critical angle Θ_{cr} as the requirement for the total internal reflection. The light incident at the interface of two media characterized by the refraction indices n_1 and n_2 meets the Snell's law condition,

$$\frac{n_1}{n_2} = \frac{\sin \Theta_2}{\sin \Theta_1} \tag{1.1}$$

where n_1 denotes the refraction index of medium 1; Θ_1 is the incident angle of light from the medium 1 on the media interface; n_2 denotes the refraction index of the medium 2; and Θ_2 is the refraction angle (Fig. 1.3.).

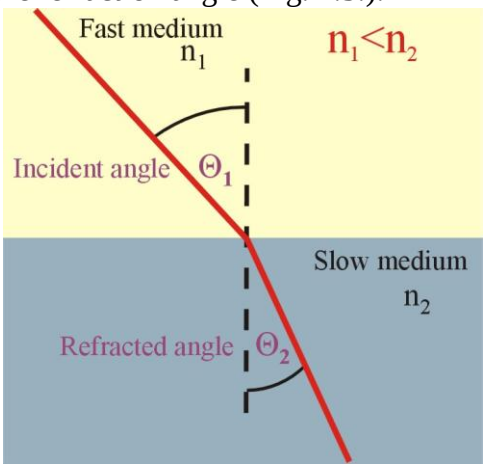

Fig. 1.3. Illustration of Snell's law.

If the light is incident on the interface from the more dense medium side (characterized by refraction index n_2) into the less dense medium (n_1) at Θ_2, the angle Θ_1 is the refraction angle. Because $n_2 > n_1$, the refraction angle Θ_1 is greater than the incident angle Θ_2. For certain critical incident angle Θ_{cr} the refraction angle is 90º. For the incident angles greater than the critical incident angle Θ_{cr}, the light is not transmitted into the less dense medium any longer. Instead, it is totally reflected at the interface (Fig. 1.4.). This phenomenon is called the total internal reflection.

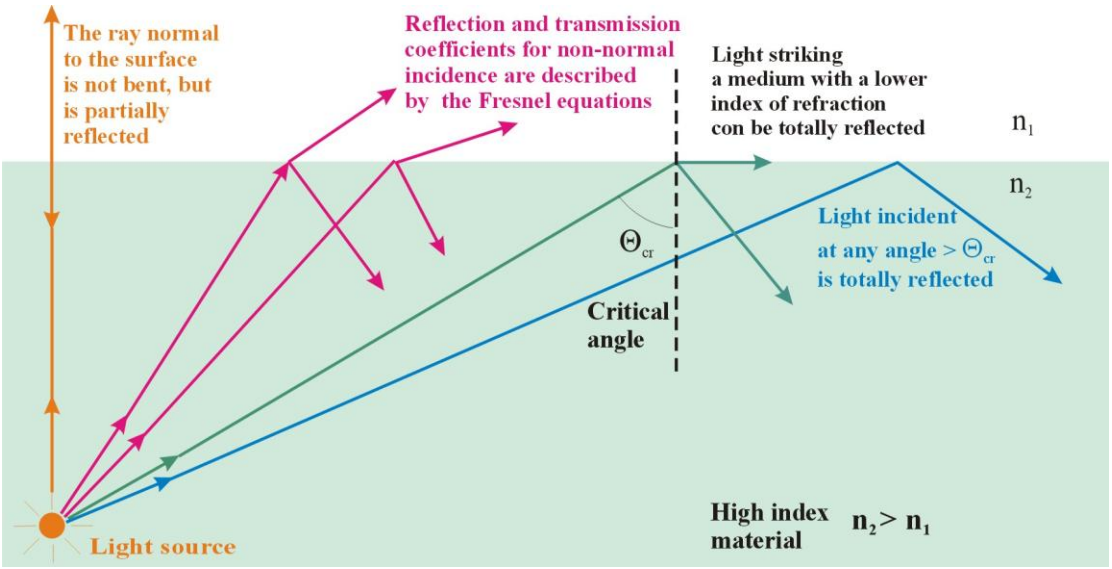

Fig. 1.4. Illustration of total internal reflection.

Fig.1.4 illustrates all possible situations, from perpendicular incidence on the interface ($\Theta_2=90^0$), through the partial reflection R_1 and partial refraction R_2 described by the Fresnel formula $R_1 / R_2 = n_2^2 / n_1^2$, the critical case (($\Theta_2=\Theta_{gr}$, $\Theta_1=90^0$), to the total internal reflection.

When the light propagates through optical fiber, Θ_{co} denotes the incident angle at the core-cladding interface, Θ_{cl} is the refraction angle, $n_1= n_{co}$ and $n_2= n_{cl}$, where n_{co} is the core refraction index and n_{cl} is the cladding refraction index (Fig.1.5).

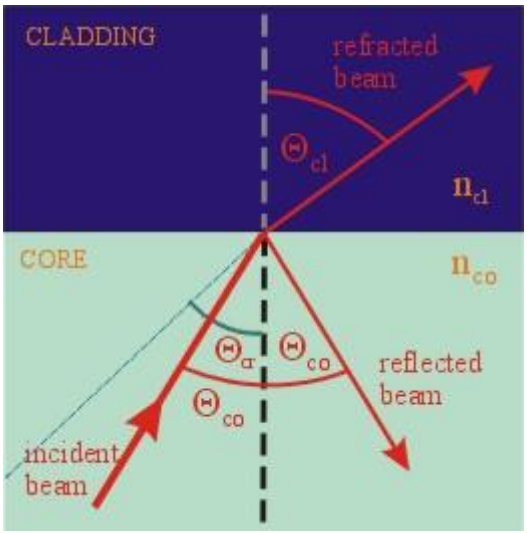

Fig.1.5. Illustration of the total internal reflection in optical fiber.

From the Snell's law we have $n_{co}\, sin\Theta_{co} = n_{cl}\, sin\Theta_{cl}$. If $\Theta_{co} \rightarrow \Theta_{cr}$ then $\Theta_{cl} \rightarrow 90^0$, which means $n_{co}\, sin\Theta_{cr} = n_{cl}\, sin90^0$, hence the critical angle Θ_{cr} for which the light is totally reflected at the interface is given by equation:

$$\Theta_{cr} = arc\ sin\{n_{cl}/n_{co}\} \tag{1.2}$$

In the total internal reflection the incident wave penetrates the less dense medium to certain depth (of the order of wavelength) which causes phase shift Φ between the incident and the reflected wave [1] :

$$tg\ \frac{\Phi}{2} = [\frac{\sin^2(\Theta_{gr})}{\sin^2\ \xi} - 1]^{1/2} \tag{1.3}$$

where $\xi = \pi/2 - \Theta$ is the angle between the optical fiber axis and the wave vector of light propagating in the waveguide (Fig.1.6.).

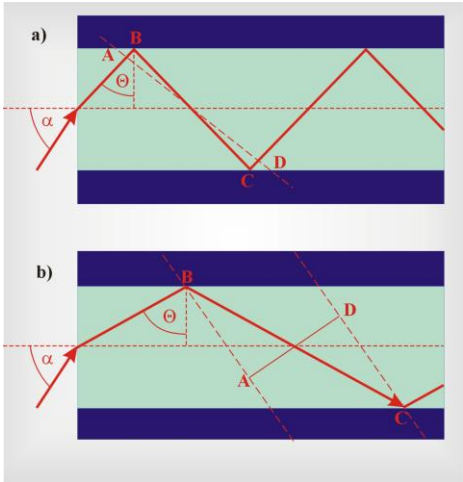

Fig. 1.6. Light propagating in the waveguide

The phase shift Φ plays an important role in light propagation in optical fiber. We will use this relation later, discussing mode types and the range of guided modes.
When the requirement of the total internal reflection is met, the ray is reflected at the core-cladding interface and returns to the core lossless, which enables light propagation through the fiber. The source of light is laser or LED diode. Electric signal on entrance is turned into optical signal in a transmitter, modulating light intensity at the same time. Near infrared radiation introduced to the optical fiber propagates in the core with the speed υ characteristic for light in given medium (that is about 200 000 000 m/s for glass, because the refraction index for a typical glass is $n \approx 1.52;\ \upsilon = \frac{c}{n}$), in order to successively get to a detector (PIN photodiode or avalanche photodiode), where the optical signal is turned back into electric signal. The schematic idea of the optical fiber transmission is shown in Fig. 1.7.

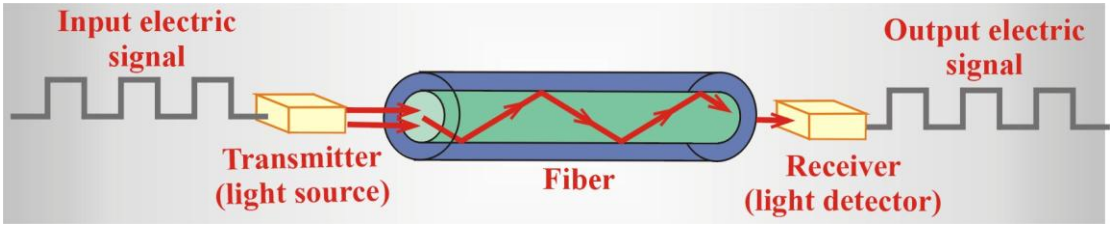

Fig. 1.7. Schematic representation of fiber optics system.

Advantages of optical fiber transmission:

- Immense binary flow rates, of the order of several Tb/s, under laboratory conditions reaching the order of 10 Tb/s, impossible while using copper based media;
- Low attenuation, the signal can be transmitted over long distances without regeneration;
- Optical fibers do not create external electromagnetic field, therefore they belong to media hard to be listened in devices;
- No inter-fiber crosstalk;
- Resistance to external electromagnetic field perturbations;
- No fire hazard;
- Bit error rate lower than 10^{-10}.

Disadvantages of optical fiber transmission:

- Higher costs than copper based media;
- Possible meltdown of the fiber at higher optical powers;
- More difficult and more expensive connections than those for copper ones.

1.3. Optical Fiber Types

We will present now different types of optical fibers applied in telecommunications, computer networks and other applications. Optical waveguides can be divided into various types considering:

a) structure (cylindrical, birefringent, planar, strip)
b) number of modes (single- or multimode fiber)
c) the refraction index profile (step-index or gradient-index fiber)
d) material (glass, plastic, semiconductor)
e) dispersion (natural dispersion, dispersion shifted fiber DSF, dispersion widened fiber DWF, reverse dispersion)
f) signal processing ability (passive – data transmission, active – amplifier)
g) polarization (classic, polarization maintaining/preserving, polarizing optical fiber)

Fig.1.8. presents cylindrical waveguide (called optical fiber), birefringent waveguide, planar waveguide, strip waveguide.

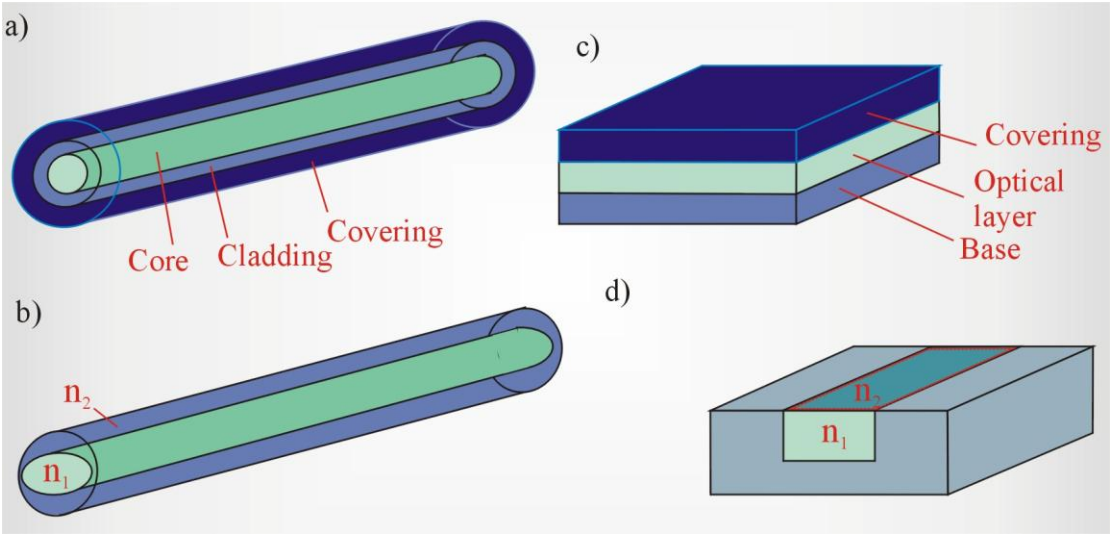

Fig.1.8. Cylindrical waveguide (a), birefringent waveguide (b), planar waveguide (c), strip waveguide (d).

Cylindrical optical fiber consists of dielectric core, most often glass, cylindrically shaped, in which light propagates. The core is surrounded by cylindrical layer of dielectric material of lower refraction index, called cladding. Typical

refraction index difference is around $n_1 - n_2 = 0.005$. The outside jacket serves a protective role.

Planar waveguide is a rectangular block consisting of three layers: base, light guide layer and coating. The base and the coating are characterized by lower refraction indices than the light propagating layer.

Considering the number of propagating modes we can divide optical fibers into **single-mode** or **multimode fibers**. The mode is one of the allowed structures of the electromagnetic field propagating through the fiber. These structures can be calculated using Maxwell equations and adequate boundary conditions. We will do it in Chapters 1.5 and 1.6.

Multimode fibers (MMF) are characterized by a large core diameter (50 or 62.5 microns) ($1\mu m=10^{-6}m$).

Single mode fibers (SMF) are characterized by a small core diameter (from 5 to 10 microns (Fig.1.9.). The cladding diameter in both cases is 125 μm.

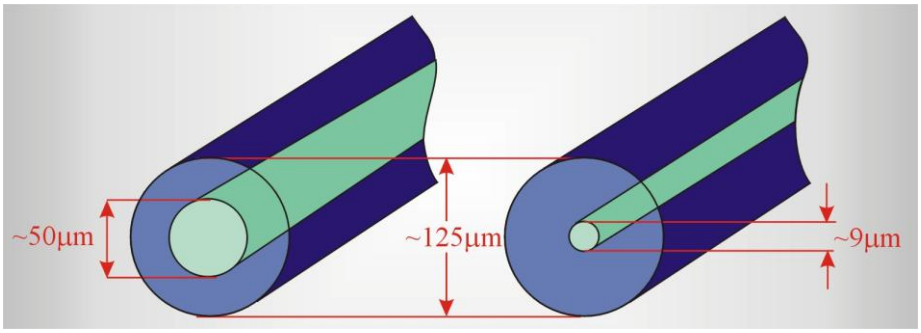

Fig.1.9. Dimensions of the multimode fiber (a) and the single mode fiber (b)

One can say intuitively that because of small core diameter, in the single mode optical fibers light propagates along one path that is nearly parallel to the fiber axis (Fig.1.10). The detailed analysis of light propagation based on the electrodynamic analysis will be provided in Chapter 1.4. We say that light wave propagates as a single mode, so-called fundamental mode, if there exists only one spatial electromagnetic field structure inside the optical fiber.

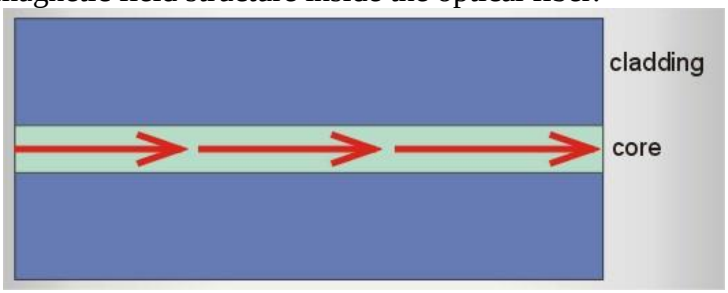

Fig.1.10. Light path in single mode fiber.

The light propagates in fiber as the single mode if the condition of υ<2.405 is met, where υ denotes normalized frequency given by the equation:

$$\upsilon = \frac{2\pi a}{\lambda_0}\sqrt{n_1^2 - n_2^2} \qquad (1.4)$$

where a is the fiber core diameter, λ_0 is the wavelength of light propagating in the fiber, n_1 and n_2 are the refraction indexes of the core and the cladding, respectively.

When the normalized frequency υ is higher – the optical fiber does not work as the single mode fiber because it propagates more modes. Condition (1.4) will be derived in Chapter 1.5, where we will provide more precise description of the electromagnetic waves propagation in dielectric fibers.
The single mode fibers do not exhibit intermodal dispersion (which will be discussed in Chapter 3), thus the light pulse reaches the end of the fiber only slightly distorted. Therefore, the single mode fiber is suitable for long-distance transmission since the light pulse can be transmitted without amplification for distance of the order of 80 – 140 km. The lack of intermodal dispersion does not mean that the pulse distortion disappear completely. Non-linear chromatic dispersion (which will be discussed in Chapter 3) as well as attenuation caused by dispersion and absorption of glass, which the core is built of, cause distortion and attenuation of the impulse along the fiber. However, this effect is weak enough, so that nowadays it is possible to transmit up to 40 Gb/s for single wavelength. The light source for single mode optical fibers is a laser emitting light of the wavelength of 1310 or 1550 nm. If, using the same single mode fiber, multiple wavelengths are sent simultaneously (WDM-wavelength division multiplexing), the transmission speed may reach the order of terabits per second (Tb/s). The techniques of multiplexing WDM will be discussed in detail in Chapter 8. The single mode fibers allow for using many protocols simultaneously, which ensures a very efficient data transfer.

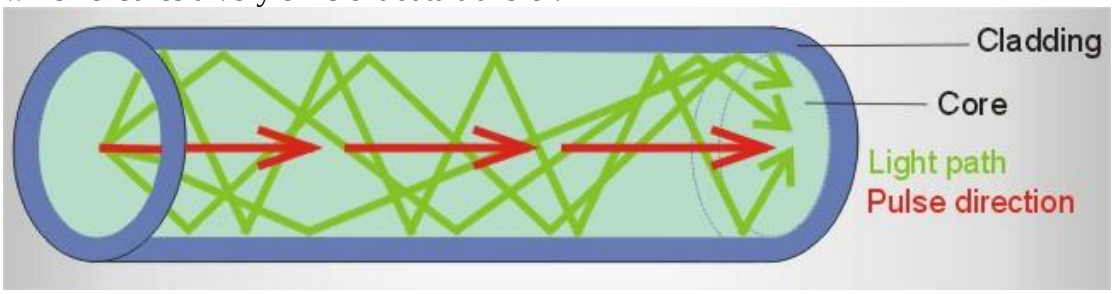

Fig.1.11. Light path in multimode optical fiber

Multimode optical fibers are characterized by large a core diameter (50/62.5 microns). The large core diameter causes that the input pulse can travel along different optical paths, showing zig-zag characteristic, which means that the travel times of rays to reach detector are different. This process leads to the temporal signal broadening This phenomenon, called intermodal dispersion leads to the temporal signal broadening and consequently limits data transfer speed and distance of effective transmission to 200 – 500 m.

The optical fibers discussed hitherto are characterized by the constant core refraction index, which exhibits a discontinuity at the core and cladding interface(Fig. 1.12.a.) and are known as the **step-index fibers.** In order to reduce the influence of the intermodal dispersion the optical fibers in which the refraction index of the core changes continuously in the direction perpendicular to fiber axis are employed (Fig. 1.12.b.). Those fibers show parabolic refraction index profile, in which the core index is described by the formula:

$$n = n_0 - \frac{1}{2} n_r r^2 \qquad (1.5)$$

and depends on a distance r from the fiber axis and $n_0 >> n_r$.

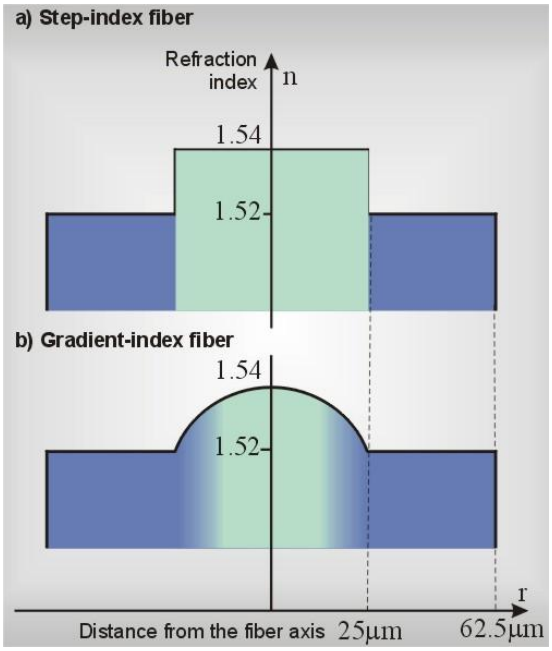

Fig. 1.12. Refraction index profile in the step-index fiber (a) and the gradient-index fiber (b)

In the gradient-index fiber the refraction index changes progressively from the core to the cladding: the refraction index of the core is the highest in the center of the core and gradually decreases approaching the core-cladding interface. Such a profiled refraction index is obtained by applying layer structure of the core. Each layer contains different admixtures, and therefore the refraction index changes continuously. Such a profiled refraction index allows for minimizing effects of the intermodal dispersion. Indeed, although different rays travel along different paths, they reach the detector approximately at the same time. This is possible since the rays propagating along the core axis in the core center (basic mode) have the shortest distance to travel, but their phase velocity is the lowest (as the refraction index is the highest in the center). The waves traveling in the layers further from the core axis have to overcome longer distance, but their phase velocity is higher due to the lower refraction index close to core-cladding interface. This means that all waves traveling along different paths reach the end of the optical fiber approximately at the same time. Thus the temporal pulse broadening caused by the intermodal dispersion is minimized. The optical fibers with the refraction index profile changing gradually, as it is shown in the Fig. 1.12.b., are known as the **gradient-index fibers**.
The geometrical ray path in such fibers does not follow a zig-zag line as it takes place in the case of the step-index fibers, it is sinusoidal, helical or axial (Fig 1.13)/

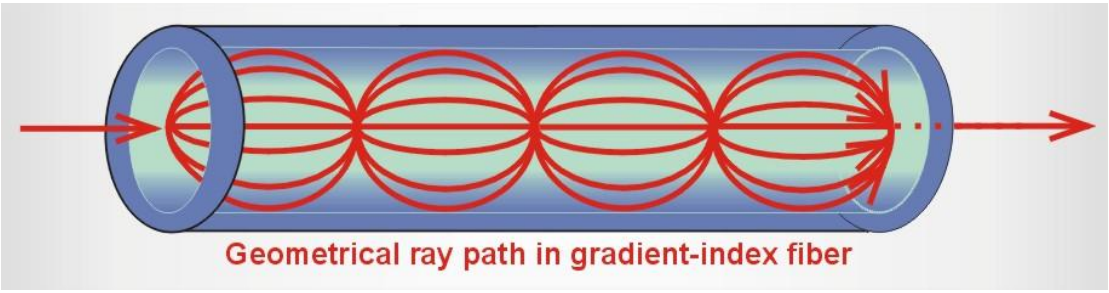

Fig. 1.13. The geometrical ray path in gradient-index fiber.

Polarization maintaining (or preserving) (**PM)** optical fibers.
In some applications maintaining constant polarization of light in an optical fiber is necessary, e.g. in fiber interferometers, fiber lasers, sensors, external fiber modulators, coherent transmission and in integrated optical circuits coupling. Besides, in all optical fibers, to lesser or higher extent, attenuation depends on polarization and deteriorates signal propagation in optical fiber. What causes change of polarization state in optical fibers? In a perfect optical fiber there is no distinguished optical axis and core and cladding materials are isotropic, therefore there is no birefringence. In real optical fibers stress, density changes, random changes of core shape or diameter cause the formation of distinguished optical axes, and result in birefringence. In consequence, two orthogonal components propagate in the optical fiber with different speeds, as ordinary and extraordinary ray. The different speeds of two orthogonal components generate phase difference changing during propagation along the fiber and random mixing of the two components causes change in polarization.

To recall, the phenomenon of birefringence can be observed while transmitting the light through certain crystals (calcite, ice, quartz, mica, sugar), which are anisotropic and have the distinguished optical axes. Light beam, while refracted, splits into two rays- ordinary and extraordinary ones that have different speeds and different refraction indices(Fig. 1.14.) This phenomenon, called double refraction or birefringence, was discovered by Bartholinus and Huygens. They found out, that both rays are linearly polarized in mutually perpendicular planes, the ordinary ray is polarized in the plane perpendicular to the plane of the optical axis. Isotropic media (fluids, gases, glasses) have only one refraction index.

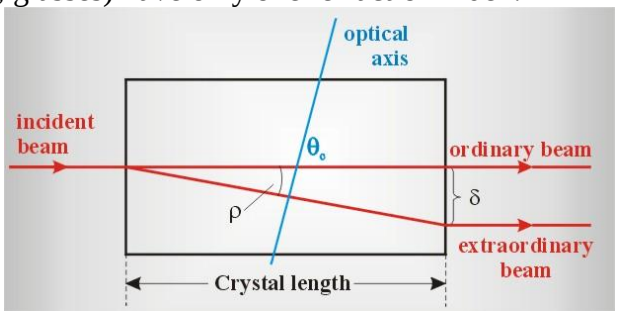

Fig. 1.14. Uniaxial birefringent crystal: o – ordinary beam, e – extraordinary beam, L – crystal length

The extraordinary beam does not satisfy Snell's Law. When we rotate the crystal about the axis perpendicular to incidence plane, we can notice that an ordinary beam stays motionless, while the extraordinary beam rotates about it. This means that the speed of light for the extraordinary beam is different for various directions depending on its orientation with respect the optical crystal axis.
We can distinguish uniaxial and biaxial crystals, and amongst them, positive and negative crystals. The cross-sections of the refraction index *n* surface for the uniaxial birefringent crystal is presented in Fig. 1.15.

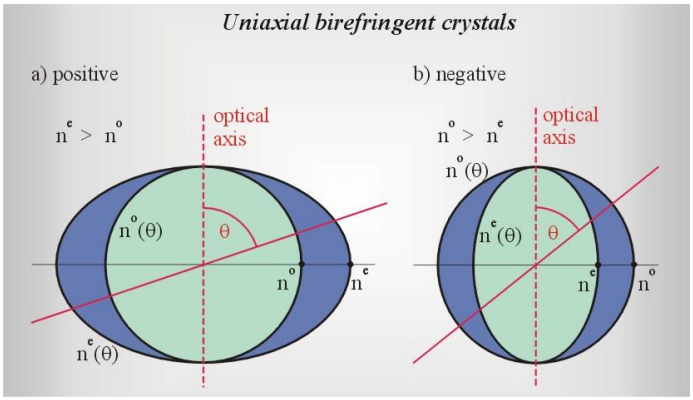

Fig. 1.15. The refractive index surface cross-sections for uniaxial birefringent crystal, a) positive, b) negative

For the ordinary ray the surface of refraction index n^0 is a sphere, because the light travels at the same speed in all directions. The extraordinary beam n^e has certain privileged propagation direction and experience the fastest propagation along the axis perpendicular to optical axis for negative crystal and along the optical axis for positive crystal.

Phase Φ for a plane wave $E = E_0 \cos(\omega t - kx)$, where $\Phi = kx$ for optical path l equals:

$$\Phi = kx = kl = \frac{2\pi}{\lambda} l = \frac{2\pi\nu n}{c} l \qquad (1.6)$$

In particular, for ordinary beam n^0 we get:

$$\Phi_o = kl = \frac{2\pi}{\lambda_o} l = \frac{2\pi\nu n^0}{c} l \qquad (1.7)$$

and for extraordinary beam n^e:

$$\Phi_e = kl = \frac{2\pi}{\lambda_e} l = \frac{2\pi\nu n^e}{c} l \qquad (1.8)$$

Therefore, the phase difference $\Delta\Phi$ equals

$$\Delta\Phi = \Phi_o - \Phi_e = \frac{2\pi\nu(n^0 - n^e)}{c} l \qquad (1.9)$$

If the phase difference for ordinary and extraordinary beam is $\Delta\Phi = \frac{\pi}{2}$, the light is circularly polarized, if the phase difference is $\Delta\Phi = \pi$, the light is polarized linearly.

In actual optical fibers microstresses give the origin for the formation of optical axes in different directions. Besides, light travels still longer path causing constant phase and polarization change. Therefore, polarization changes chaotically in time.

In order to maintain polarization two opposite methods can be chosen:

- using asymmetric, anisotropic stress in glaze to maximize controlled birefringence. This method is used in **high birefringence (HB)** optical fibers.
- using perfectly symmetric, isotropic fibers, to minimize birefringence. This method is used in **low birefringence (LB)** optical fibers. The fiber must be

characterized by low stresses, ideal geometry and homogenous density distribution along the axis.

- using polarization analyzers, which will pass only certain polarization.

In polarization maintaining (PM) fiber, in which birefringence was intentionally created, polarization state does not change chaotically. The distinguished optical axis causes that random changes of density fluctuation and temporary changes of optical axis become negligible and are masked by main effect - intentionally created birefringence. When the light polarization coincides with optical axis (or the axis parallel to it) polarization state does not change over long distances. However, if the optical axis is at an angle to polarization direction, two orthogonal components are created: slow (in negative crystal it corresponds to an extraordinary beam) and fast beam (ordinary), which, for longer optical distances, generate periodically changing phase difference. Thus, for 45º angle, first we observe linear polarization, followed by elliptical and circular polarization (with phase difference $\Delta\Phi = \frac{\pi}{2}$**),** subsequently again linear ($\Delta\Phi = \pi$), but perpendicular to the linear polarization at entrance, elliptical, circular ($\Delta\Phi = \frac{3\pi}{2}$), in order to return to initial polarization after a full period ($\Delta\Phi = 2\pi$). For longer distances the cycle repeats. Fig. 1.16. shows the evolution of polarization state in polarization maintaining fiber, in case when the input signal is linearly polarized at 45º from a slow optical axis.

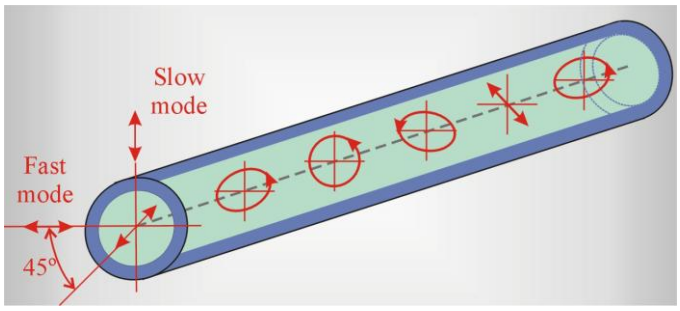

Fig.1.16. Evolution of state of polarization along a polarization maintaining fiber, when the input signal is linearly polarized at 45° from the slow axis.

The measure of birefringence is parameter called modal birefringence B_m (which symbol should not be mistaken for normalized propagation constant) defined by equation:

$$B_m = \frac{\left|\beta_y - \beta_x\right|}{k_0} = n_{ef}^x - n_{ef}^y, \qquad (1.10)$$

where β_y and β_x are propagation constants of orthogonal modes, whereas n_{ef}^x and n_{ef}^y are effective refraction indexes for directions *x* and *y*, k_0 is a wave vector. Typical values $B_m \approx 10^{-6}$ for LB fibers and $B_m \approx 10^{-6}$ for high birefringence fibers (HB).
Another parameter defining birefringence of fiber is a beat length defined as

$$L_B = \frac{2\pi}{\left|\beta_y - \beta_x\right|}, \qquad (1.11)$$

where L_B is the distance necessary for the increase of orthogonal modes difference by $\frac{\pi}{2}$, the distance of power exchange between modes. This phenomenon repeats periodically.

Fig. 1.17. presents typical cross-section of polarization maintaining fiber. We can notice on the cross-section, in the fiber, next to the core, there are two openings, which are filled with stress rods made of material characterized by higher thermal expansion coefficient than cladding. After fiber drawing, stresses are created along the distinguished axis in the waveguide, which cause controlled birefringence. Therefore, the fiber acts as polarization analyzer and transmits the light in only one polarization plane.

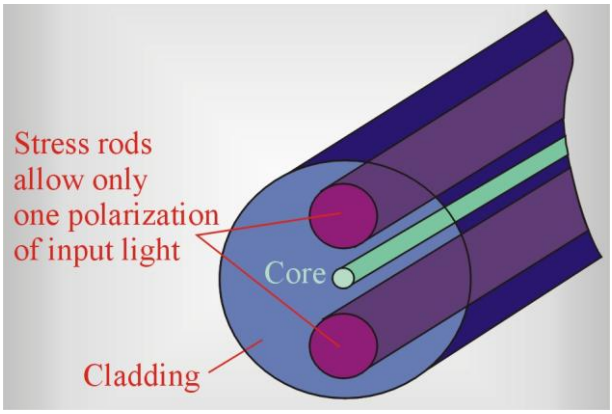

Fig. 1.17. Cross-section of polarization maintaining fiber.

Other types of fibers, among them dispersion shifted fibers, will be discussed in a chapter devoted to dispersion in optical fibers. In order to understand their operation principals we need to understand non-linear optical effects occurring in fibers. Here we only are going to mention, that non-linear effects are highly disadvantageous in long-distance fiber optics transmissions, they lead to spreading out of time impulse, and in consequence, crosstalk between channels in wavelength-division multiplexing (WDM) techniques and limitations in optical fiber throughput.

Dispersion Shifted-Single Mode Fiber (DS-SMF) are characterized by gradient profile of refractive index, strongly negative dispersion in II transmission window (below 20 ps/nm·km) and zero dispersion for 1550 nm in III window. Their main application is a single-channel long distance transmission in III window. They are not applicable for multi-channel transmission, because the lack of dispersion causes crosstalks due to other nonlinear effect: four wave mixing (FWM). Therefore, in order to reduce nonlinear dispersion and, at the same time, exclude four wave mixing, **Non Zero Dispersion Shifted-Single Mode Fibers (NZDS-SMF)**, which are characterized by low, but non-zero dispersion for whole transmission range of optical amplifiers EDFA (1530-1565 nm), were introduced. Low, but non-zero dispersion limits nonlinear effects of FWM and cross-phase modulation (CPM) and is thus far the best medium with application of multiplexing in transmission DWDM (dense wavelength division multiplexing) in III transmission window over long distances.

Fig. 1.18. illustrates different types of single mode fibers with shifted dispersion applied in III optical window, 1550 nm. The region marked in blue denotes EDFA (Erbium Doped Fiber Amplifier) window and represents the wavelengths currently used in multiplexing techniques DWDM.

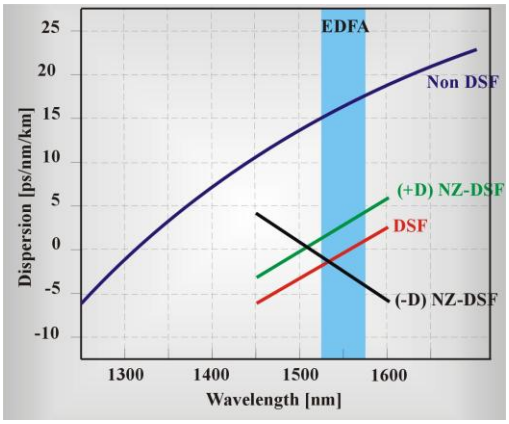

Fig. 1.18. Different types of Dispersion Shifted-Single Mode Fiber.

- single mode fibers without shifted dispersion (Non-DSF): zero dispersion GVD for 1310 nm
- single mode fibers with shifted dispersion (DSF): zero dispersion GVD occurs for 1550 nm, application in single-channel TDM (Time Division Multiplexing), nonlinear effects cause problems for multi-channel techniques DWDM
- single mode fibers with non zero shifted dispersion with positive inclination of D coefficient (+D) NZ-DSF: fibers similar to DSF, however zero dispersion is moved outside 1550 nm window. For 1550 nm the fiber is characterized by low, but non-zero dispersion GVD, the inclination of D wavelength coefficient is positive
- single mode fibers with non zero shifted dispersion with negative inclination of D coefficient (-D) NZ-DSF: fibers similar to DSF, however zero dispersion is moved outside 1550 nm window. For 1550 nm the fiber is characterized by low, but non-zero dispersion GVD, the inclination of D wavelength coefficient is negative.

1.4. Propagation Of Light In Optical Fibers. Electrodynamic Analysis.

1.4.1. Step-Index Cylindrical Fiber

Propagation of light in optical fibers is described by Maxwell equations, similarly to all other electromagnetic phenomena. The wave equation derived from the Maxwell equations describes propagation of light in optical fiber. If we make the following assumptions:

- nonlinear polarization is negligible,
- we can neglect the imaginary component of dielectric constant $\varepsilon(\omega) = (n(\omega) + i\alpha c / 2\omega)^2$, because the loss in optical fiber is low in spectrum range of interest for fiber optics techniques, therefore $\alpha \approx 0$,
- refractive index $n(\omega)$ does not depend on core and cladding spatial coefficients (Fig. 1.12.a.), as it is in the case of step-index fibers,

then the wave equation takes form of equation known as Helmholtz equation

$$\nabla^2 \tilde{\boldsymbol{E}} + n^2(\omega) k_0^2 \tilde{\boldsymbol{E}} = 0 \qquad (1.12)$$

In Cartesian coordinate system Laplace operator is expressed as follows:

$$\nabla^2 = \frac{\partial^2}{\partial x^2} + \frac{\partial^2}{\partial y^2} \frac{\partial^2}{\partial z^2} \qquad (1.13)$$

where $k_0 = \frac{\omega}{c} = \omega\sqrt{\mu_0\varepsilon_0}$ is the wave vector length (wave number), μ_0 and ε_0 denote magnetic and dielectric permeability of free space, $\tilde{\boldsymbol{E}} = \tilde{\boldsymbol{E}}(\boldsymbol{r}, \omega)$ is Fourier transform of electric field

$$\tilde{\boldsymbol{E}}(\boldsymbol{r}, \omega) = \int_{-\infty}^{+\infty} \boldsymbol{E}(\boldsymbol{r}, t)\, exp(i\omega t)dt \qquad (1.14)$$

Propagation of light and mode analysis is described in details in numerous handbooks [2-9]. Let us consider the solution of equation (1.12). Equation (1.12) is a vector equation, therefore it is an equivalent of three differential scalar equation for three electric field $\boldsymbol{E}$ components. In Cartesian coordinate system those are E_x, E_y, E_z and this description is most proper for planar waveguides (Fig. 1.8.). For optical fibers, most commonly used in telecommunications, it is most convenient to use polar coordinates (r, Φ, z) because of cylindrical symmetry of optical fibers. Then, Equation (1.12) takes the following form:

$$\frac{\partial^2 \tilde{\boldsymbol{E}}}{\partial r^2} + \frac{1}{r}\frac{\partial^2 \tilde{\boldsymbol{E}}}{\partial r^2} + \frac{1}{r^2}\frac{\partial^2 \tilde{\boldsymbol{E}}}{\partial \phi^2} + \frac{\partial^2 \tilde{\boldsymbol{E}}}{\partial z^2} + n^2 k_0^2 \tilde{\boldsymbol{E}} = \boldsymbol{0} \qquad (1.15)$$

Cartesian and polar coordinates are linked as follows: $x = r\cos\phi$, $y = r\cos\phi$, $z = z$

Similar equation can be written for magnetic field strength $\tilde{\boldsymbol{H}}$. Full solution must therefore contain six components, however, taking into account four Maxwell equations, only two components are independent. Let us choose $\tilde{E}_z$ and $\tilde{H}_z$ ad independent components. Assuming that the *z* axis overlaps with optical fiber axis, we obtain the following scalar equation for electric field E_z component along the fiber axis:

$$\frac{\partial^2 \tilde{\boldsymbol{E}}_z}{\partial r^2} + \frac{1}{r}\frac{\partial^2 \tilde{\boldsymbol{E}}_z}{\partial r^2} + \frac{1}{r^2}\frac{\partial^2 \tilde{\boldsymbol{E}}_z}{\partial \phi^2} + \frac{\partial^2 \tilde{\boldsymbol{E}}_z}{\partial z^2} + n^2 k_0^2 \tilde{\boldsymbol{E}}_z = \boldsymbol{0} \qquad (1.16)$$

Of course, the fact, that the electric field component $\tilde{E}_z$ is directed along the fiber axis does not imply, that the electromagnetic wave seizes to be a transverse wave. The wave propagating in a fiber can show any polarization, which can be depicted as superposition of waves having their vectors in two mutually perpendicular planes (denoted as *s* and *p* polarization). Transverse magnetic (TM) waves, which electric field vector shows *s* polarization (in the plane of Fig. 1.19, which incorporates fiber axis as well), are characterized with non-zero electric field intensity $E_z \neq 0$, along the fiber axis *z*, whilst magnetic field component $H_z = 0$.

On the contrary, in the case of transverse electric (TE) waves, electric field vector shows *p* polarization (in the plane perpendicular to that of Fig. 1.14), $E_z = 0$, whilst $H_z \neq 0$. Fig. 1.19. depicts only one of the possible propagation planes of beam incident to and refracted at core-cladding interface. It means, that besides the cases shown in Fig. 1.19., there are modes having non-zero components of both fields $E_z \neq 0$, $H_z \neq 0$ along the fiber axis *z*. Such modes are called hybrid and denoted EH and HE.

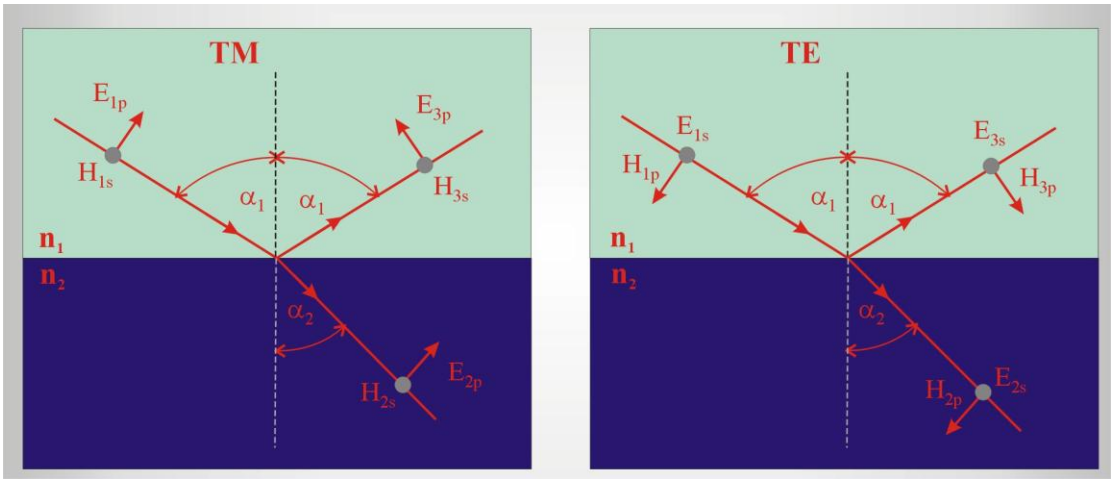

Fig. 1.19. Illustration of TM and TE modes. Index p *denotes electric field intensity vector in the plane incorporating fiber axis,* s *– perpendicular to this plane.*

Let us apply the method of variable separation to solve the equation (1.16). we will be looking for the solution in a form:

$$\tilde{E}_z = R(r)\Phi(\phi)Z(z) \tag{1.17}$$

Substituting equation (1.17) to (1.16) and dividing both sides of equation (1.16) by $R(r)\Phi(\phi)Z(z)$ we obtain:

$$\frac{1}{Z}\frac{d^2Z}{dz^2} = -\left(\frac{1}{R}\frac{d^2R}{dr^2} + \frac{1}{Rr}\frac{dR}{dr} + \frac{1}{r^2\Phi}\frac{d^2\Phi}{d\phi^2} + n^2k_0^2\right) \tag{1.18}$$

As we can see, right side of the equation does not depend on z, therefore the changes along fiber axis *z* do not influence the right side of the equation. This means, that the left side of the equation must be a certain constant (in general, a complex constant).

Let us denote this constant as γ^2, where

$$\gamma = \alpha + i\beta \tag{1.19}$$

As we expect the solution of equation in form of oscillating wave, therefore β must denote phase constant and is named propagation constant, while α describes attenuation (and oscillating wave fading away) in optical fiber. As the attenuation in optical fiber is low, we can assume with good approximation α=0. The problem of attenuation will be discussed in Chapter 3. Therefore

$$\frac{1}{Z}\frac{d^2Z}{dz^2} = \gamma^2 \tag{1.20}$$

The solution of equation (1.20) is well known function

$$Z(z) = C_1\,exp(-\gamma z) + C_2\,exp(\gamma z) \tag{1.21}$$

representing waves propagating in opposite directions along the fiber axis, where C_1 and C_2 are the constants determined from boundary conditions. In further discussion we will consider only the wave propagating in the positive direction, making the assumption C_2=0. Solving the right side of equation (1.18) we obtain:

$$\frac{1}{\Phi}\frac{d^2\Phi}{d\phi^2} = -\left(\frac{r^2}{R}\frac{d^2R}{dr^2} + \frac{r}{R}\frac{dR}{dr} + r^2\gamma^2 + r^2n^2k_0^2\right) \tag{1.22}$$

Right side of this equation does not depend on Φ, thus the left side of the equation must be equal to a certain constant, which we will denote as $-m^2$. Therefore we get

$$\Phi(\phi) = C_3\,cos(m\phi) + C_4\,sin(m\phi) \tag{1.23}$$

where C_3 and C_4 are the constants determined from boundary conditions. Function $\Phi(\phi)$ must meet the condition of rotational symmetry, $\Phi(\phi) = \Phi(\phi + 2\pi)$, therefore m in equation (1.23) must be an integer. Finally, substituting γ^2 and m^2 constants into equation (1.18) we get

$$\frac{d^2R}{dr^2} + \frac{1}{r}\frac{dR}{dr} + (h^2 - \frac{m^2}{r^2})R = 0 \qquad (1.24)$$

where

$$h^2 = \gamma^2 + n^2 k_0^2 \qquad (1.25)$$

The solution of equation (1.24) should exhibit oscillatory character in the core and decaying in the cladding. In order for this condition to be met, h must be a real number in the core, and imaginary number in the cladding, that is:

$h = h_1$ for $r<a$ and $h = ih_2$ for $r>a$ (1.25.a)

The solution for ordinary differential equation (1.24) for $h = h_1$, that is in the core, are **Bessel functions**.

$$R(r) = C_5 J_m(h_1 r) + C_6 N_m(h_1 r) \quad \text{for} \quad r<a \qquad (1.26)$$

Function J_m is a Bessel function of the first kind, N_m is a Bessel function of the second kind and m order and is called Neumann function.

Figures 1.20. and 1.21. depict Bessel functions of first and second kind. For $r \to 0$ N_m function approach minus infinity, and has no physical meaning. We can avoid it only if we assume that C_6=0. Substituting equations (1.21), (1.23) and (1.26) to (1.17) we obtain

$$\tilde{E}_z = J_m(h_1 r)(A_1 \cos m\phi + B_1 \sin m\phi) \exp(-\gamma z) \quad r<a \qquad (1.27)$$

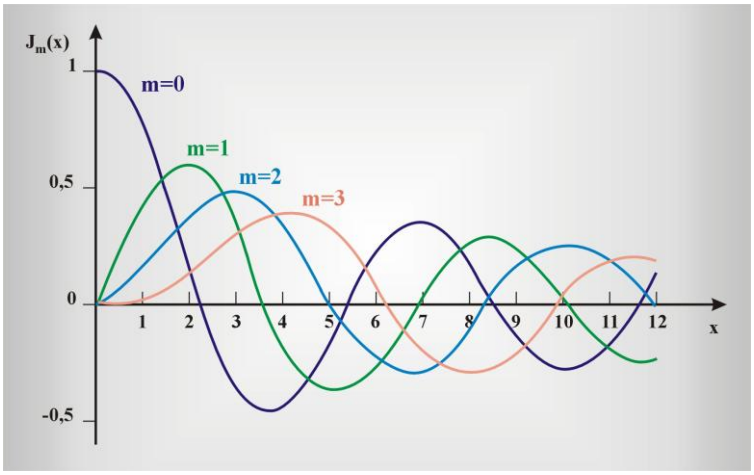

Fig. 1.20. Bessel function of the first kind and m *order*

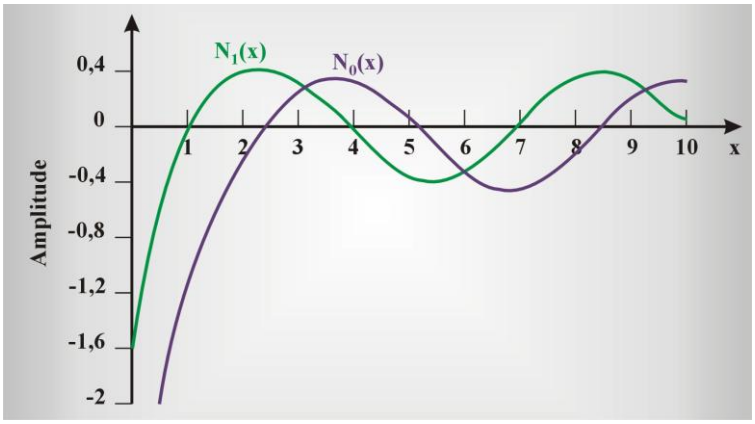

Fig. 1.21. Bessel function of the second kind and m *order (Neumann functions)*

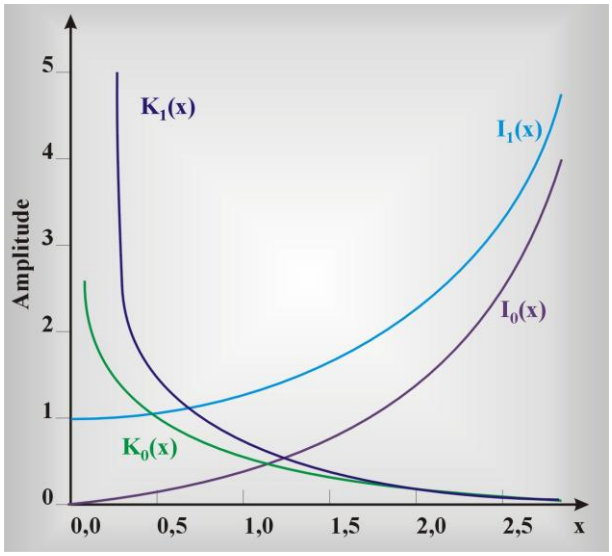

Rys. 1.22. Modified Bessel functions of the first and the second kind and m *order*

Using the denotation (1.25.a) Bessel equation (1.24) for the core takes form

$$\frac{d^2R}{dr^2} + \frac{1}{r}\frac{dR}{dr} - (h_2^2 + \frac{m^2}{r^2})R = 0 \qquad r>a \qquad (1.28)$$

and its solution is

$$R(r) = C_7 I_m(h_2 r) + C_8 K_m(h_2 r) \qquad (1.29)$$

Function I_m is a modified Bessel function of the first kind, function K_m is a modified Bessel function of the second kind and *m* order.

Fig. 1.22. shows Bessel functions of the first and the second kind. For $r\to\infty$ N_m function approach infinity, and has no physical meaning. We can avoid it only assuming that C_7=0. Substituting equations (1.21), (1.23) and (1.29) to (1.17) we get

$$\tilde{E}_z = K_m(h_2 r)(A_2 \cos m\phi + B_2 \sin m\phi)\exp(-\gamma z) \qquad r>a \qquad (1.30)$$

Following the similar procedure for magnetic field intensity vector *H* we can prove [5], that *z* component of magnetic field $\tilde{H}_z$ along the fiber axis equals

$$\tilde{H}_z = J_m(h_1 r)(F_1 \cos m\phi + G_1 \sin m\phi)\exp(-\gamma z) \qquad r<a \qquad (1.31)$$

$$\tilde{H}_z = K_m(h_2 r)(F_2 \cos m\phi + G_2 \sin m\phi)\exp(-\gamma z) \qquad r>a \qquad (1.32)$$

where F_1 , G_1, F_2, G_2 are the constants which can be determined from boundary conditions.

Having determined two independent components $\tilde{E}_z$ and $\tilde{H}_z$ further four components can be calculated from Maxwell equations

$$\nabla \times E = -i\omega\mu H \tag{1.33}$$

$$\nabla \times H = i\omega\varepsilon E \tag{1.34}$$

where the rotation operator in cylindrical coordinates is given by the following formula:

$$\nabla \times A = \begin{vmatrix} \frac{i_z}{r} & \frac{i_r}{r} & i_\phi \\ \frac{\partial}{\partial_z} & \frac{\partial}{\partial_r} & \frac{\partial}{\partial_\phi} \\ A_z & A_r & A_\phi \end{vmatrix} \tag{1.35}$$

Using equations (1.33)-(1.35) we get

$$\tilde{E}_r = -\frac{1}{h^2}\left(\gamma \frac{\partial \tilde{E}_z}{\partial_r} + \frac{i\omega\mu}{r}\frac{\partial \tilde{H}_z}{\partial\phi}\right) \tag{1.36}$$

$$\tilde{E}_\phi = \frac{1}{h^2}\left(-\frac{\gamma}{r}\frac{\partial \tilde{E}_z}{\partial\phi} + i\omega\mu \frac{\partial \tilde{H}_z}{\partial_r}\right) \tag{1.37}$$

$$\tilde{H}_r = \frac{1}{h^2}\left(\frac{i\omega\varepsilon}{r}\frac{\partial \tilde{E}_z}{\partial\phi} - \gamma \frac{\partial \tilde{H}_z}{\partial r}\right) \tag{1.38}$$

$$\tilde{H}_\phi = -\frac{1}{h^2}\left(i\omega\varepsilon \frac{\partial \tilde{E}_z}{\partial r} + \frac{\gamma}{r}\frac{\partial \tilde{H}_z}{\partial\phi}\right) \tag{1.39}$$

1.4.2. Type TE (Or H) Modes

Let us consider TE type modes (Fig. 1.19.) first. For TE type modes we substitute $\tilde{E}_z = 0$, and $\tilde{H}_z \neq 0$ in the direction z of the fiber axis, as formulated by equations (1.31)-(1.32) to (1.39) and we obtain

$$\tilde{H}_\phi = \frac{m\gamma}{h_1^2 r} J_m(h_1 r)(F_1 \sin m\phi - G_1 \cos m\phi) \exp(-\gamma z) \qquad r<a \tag{1.40}$$

$$\tilde{H}_\phi = -\frac{m\gamma}{h_2^2 r} K_m(h_2 r)(F_2 \sin m\phi - G_2 \cos m\phi) \exp(-\gamma z) \qquad r>a \tag{1.41}$$

rom the condition of $\tilde{H}_z$ field continuity at the core-cladding interface from equations (1.31) and (1.32) we get

$$F_1 J_m(u) = F_2 K_m(w) \tag{1.42}$$

where: $u = h_1 a$, $w = h_2 a$ (1.43)

and *a* is the core diameter.

From the condition of $\tilde{H}_\phi$ field continuity at the core-cladding interface from equations (1.40) and (1.41) we get

$$-\frac{F_1}{h_1^2} J_m(u) = \frac{F_2}{h_2^2} K_m(\mathrm{w}) \tag{1.44}$$

As values F_1 and F_2 are positive, equations (1.42) and (1.44) are not contradictory only for *m*=0, since then $\tilde{H}_\phi$=0 and the condition of $\tilde{H}_\phi$ field continuity is no longer valid.

For *m*=0 $\tilde{H}_z$ component from equations (1.31) and (1.32) takes form

$$\tilde{H}_z = F_1 J_0(h_1 r)\, exp(-\gamma z) \quad r<a \qquad (1.45)$$

$$\tilde{H}_z = F_2 K_0(h_2 r)\, exp(-\gamma z) \quad r>a \qquad (1.46)$$

Substituting equations (1.45) and (1.46) to (1.38) we get

$$\tilde{H}_r = -\frac{\gamma}{h_1} F_1 \frac{dJ_0(h_1 r)}{dr} exp(-\gamma z) \quad r<a \qquad (1.47)$$

$$\tilde{H}_r = \frac{\gamma}{h_2} F_2 \frac{dK_0(h_2 r)}{dr} exp(-\gamma z) \quad r>a \qquad (1.48)$$

Moreover, as it can be seen from equations (1.45) and (1.46), $\tilde{H}_z$ does not depend on Φ and $\tilde{E}_z$ =0, from equation (1.36) we obtain $\tilde{E}_r$ =0.

Following analogous procedure we can determine $\tilde{E}_\phi$ component via substitution of equations (1.45) and (1.46) to (1.37)

$$\tilde{E}_\phi = \frac{1}{h_1} F_1 i\omega\mu_0 \frac{dJ_0(h_1 r)}{dr} exp(-\gamma z) \quad r<a \qquad (1.49)$$

$$\tilde{E}_\phi = -\frac{1}{h_2} F_2 i\omega\mu_0 \frac{dK_0(h_2 r)}{d_r} exp(-\gamma z) \quad r>a \qquad (1.50)$$

From the condition of $\tilde{E}_\phi$ and $\tilde{H}_r$ fields continuity at the core-cladding interface we get

$$\frac{1}{h_1} F_1 J_0'(u) = -\frac{1}{h_2} F_2 K_0'(\omega) \qquad (1.51)$$

and therefore **the characteristic equation** for TE (or H) type modes

$$\frac{1}{u}\frac{J_0'(u)}{J_0(u)} = -\frac{1}{w}\frac{K_0'(w)}{K_0(w)} \qquad (1.52)$$

where F_1 and F_2 constants were eliminated using equations (1.51) and (1.42).

Assuming that the expression (1.19) takes form $\gamma = i\beta$ (when attenuation is negligible $\alpha \approx 0$) relation (1.25) can be written as

$$h_1^2 = -\beta^2 + k_0^2 n_1^2 \quad r<a \qquad (1.53)$$

$$-h_2^2 = -\beta^2 + k_0^2 n_2^2 \quad r>a \qquad (1.54)$$

Multiplying the above equations by core diameter *a* and subtracting the respective sides of equations we get:

$$\upsilon^2 = u^2 + w^2 \qquad (1.55)$$

where

$$\upsilon = \frac{2\pi a}{\lambda_0}\sqrt{n_1^2 - n_2^2} \qquad (1.56)$$

The quantity υ in expression (1.56) is named normalized frequency, and

$$k_0 = \frac{2\pi}{\lambda_0} \qquad (1.56.a)$$

Physical meaning of the quantity expressed by equation (1.56) we will understand later.

To sum up, for TE type waves we obtain the following field components

$$\begin{aligned}
&\tilde{E}_z = 0 && r<a \\
&\tilde{E}_z = 0 && r>a \\
&\tilde{H}_z = F_1 J_0(h_1 r)\exp(-\gamma z) && r<a \\
&\tilde{H}_z = F_2 K_0(h_2 r)\exp(-\gamma z) && r>a \qquad (1.57)\\
&\tilde{H}_r = -\frac{\gamma}{h_1} F_1 \frac{dJ_0(h_1 r)}{dr}\exp(-\gamma z) && r<a \\
&\tilde{H}_r = \frac{\gamma}{h_2} F_2 \frac{dK_0(h_2 r)}{dr}\exp(-\gamma z) && r>a
\end{aligned}$$

1.4.3. Type TH (Or E) Modes

Following analogous procedure for type TM (E) waves, for which H_z=0, we obtain **the characteristic equation** [5,7]

$$\frac{\varepsilon_1}{u}\frac{J_0'(u)}{J_0(u)} = -\frac{\varepsilon_2}{w}\frac{K_0'(w)}{K_0(w)} \qquad (1.58)$$

where ε_1 and ε_2 are dielectric permittivities of core and cladding.

1.4.4. Hybrid Modes EH And HE

The only modes left for consideration are HE and EH, having non-zero components it the wave propagation direction. Substituting *z* components of electric and magnetic field (1.27), (1.30), (1.45), (1.46) to equation (1.37) we obtain [5,7]

$$E_\phi = \frac{1}{h_1^2}\left[-\frac{\gamma}{r} J_m(h_1 r)(-A_1 m \sin m\phi + B_1 m \cos m\phi) + \right. \qquad r<a \qquad (1.59)$$
$$\left. + i\omega\mu_0 h_1 J_m'(h_1 r)(F_1 \cos m\phi + G_1 \sin m\phi)\right]\exp(-\gamma z)$$

$$\tilde{E}_\phi = -\frac{1}{h_2^2}\left[-\frac{\gamma}{r} K_m(h_2 r)(-A_2 m \sin m\phi + B_2 m \cos m\phi) + \right. \qquad r>a \qquad (1.60)$$
$$\left. + i\omega\mu_0 h_2 K_m'(h_2 r)(F_2 \cos m\phi + G_2 \sin m\phi)\right]\exp(-\gamma z)$$

From the condition of E_ϕ component continuity at the core-cladding interface we get

$$
\begin{aligned}
&\sin m\phi\{\frac{1}{h_1^2}\,[\frac{m\gamma}{a}\,A_1 J_m(u) + i\omega\mu_0 h_1 G_1 J_m'(u)] + \\
&+\frac{1}{h_2^2}\,[m\,\frac{\gamma}{a}\,A_2 K_m(w) + i\omega\mu_0 h_2 G_2 K_m'(w)]\} + \\
&+\cos m\phi\{\frac{1}{h_1^2}\,[-\frac{m\gamma}{a}\,B_1 J_m(u) + i\omega\mu_0 h_1 F_1 J_m'(u)] + \\
&+\frac{1}{h_2^2}\,[-m\,\frac{\gamma}{a}\,B_2 K_m(w) + i\omega\mu_0 h_2 F_2 K_m'(w)]\} = 0
\end{aligned}
\tag{1.61}
$$

Because relation (1.61) must be fulfilled for each angle ϕ therefore the arguments of trigonometric functions must equal to zero.
We can distinguish the following cases:

1) All constants in equation (1.61) equal to zero, which corresponds to trivial solution,
2) $B_1 = B_2 = F_1 = F_2 = 0$, which corresponds to non-trivial solution, with non-zero values $A_1 = A_2 = G_1 = G_2$,
3) $A_1 = A_2 = G_1 = G_2 = 0$, which corresponds to non-trivial solution, with non-zero values $B_1 = B_2 = F_1 = F_2$.

The cases 2) i 3) describe mutually perpendicular solutions. They correspond to hybrid modes HE and EH.
For the case 2) we obtain [5, 7] the following field components of hybrid type HE and EH

$$\tilde{E}_z = A_1 J_m(h_1 r)\cos m\phi\, \exp(-\gamma z) \qquad r<a \tag{1.62}$$

$$\tilde{E}_z = A_2 K_m(h_2 r)\cos m\phi\, \exp(-\gamma z) \qquad r>a \tag{1.63}$$

$$\tilde{H}_z = G_1 J_m(h_1 r)\sin m\phi\, \exp(-\gamma z) \qquad r<a \tag{1.64}$$

$$\tilde{H}_z = G_2 K_m(h_2 r)\sin m\phi\, \exp(-\gamma z) \qquad r>a \tag{1.65}$$

$$\tilde{E}_\phi = \frac{1}{h_1^2}\left[\frac{m\gamma}{r}\,A_1 J_m(h_1 r) + i\omega\mu_0 h_1 G_1 J_m'(h_1 r)\right]\sin m\phi\, \exp(-\gamma z) \qquad r<a \tag{1.66}$$

$$\tilde{E}_\phi = -\frac{1}{h_2^2}\left[\frac{m\gamma}{r}\,A_2 K_m(h_2 r) + i\omega\mu_0 h_2 G_2 K_m'(h_2 r)\right]\sin m\phi\, \exp(-\gamma z) \qquad r>a \tag{1.67}$$

$$\tilde{E}_r = -\frac{1}{h_1^2}\left[\gamma h_1 A_1 J_m'(h_1 r) + \frac{i\omega\mu_0 m}{r}\,G_1 J_m(h_1 r)\right]\cos m\phi\, \exp(-\gamma z) \qquad r<a \tag{1.68}$$

$$\tilde{E}_r = \frac{1}{h_2^2}\left[\gamma h_2 A_2 K_m'(h_2 r) + \frac{i\omega\mu_0 m}{r}\,G_2 K_m(h_2 r)\right]\cos m\phi\, \exp(-\gamma z) \qquad r>a \tag{1.69}$$

The correlations between constants can be found from the condition of $\tilde{E}_z$ and $\tilde{H}_z$ field continuity

$$A_2 = A_1 \frac{J_m(u)}{K_m(w)} \tag{1.70}$$

$$G_2 = G_1 \frac{J_m(u)}{K_m(w)} \tag{1.71}$$

The condition of $\tilde{E}_\phi$ field continuity provides the correlation [5,12]

$$\frac{1}{h_1^2}\left[\frac{m\gamma}{a} A_1 J_m(u) + i\omega\mu_0 h_1 G_1 J_m(u)\right] = \\ = -\frac{1}{h_2^2}\left[\frac{m\gamma}{a} A_2 K_m(w) + i\omega\mu_0 h_2 G_2 K_m'(w)\right] \tag{1.72}$$

,

whereas the condition of continuity of normal component of electric induction εE takes form [5,12]

$$-\frac{\varepsilon_1}{h_1^2}\left[\gamma h_1 A_1 J_m'(u) + \frac{i\omega\mu_0 m}{a} G_1 J_m(u)\right] = \\ = \frac{\varepsilon_2}{h_2^2}\left[\gamma h_2 A_2 K_m'(w) + \frac{i\omega\mu_0 m}{a} G_2 K_m(w)\right] \tag{1.73}$$

Expressing A_2 and G_2 using equations (1.70) and (1.71), and assuming, that equation (1.19) takes form $\gamma = i\beta$ (when attenuation is negligible $\alpha \approx 0$) we obtain

$$\left(\frac{1}{u^2} + \frac{1}{w^2}\right) m\beta A_1 + \left[\frac{1}{u}\frac{J_m'(u)}{J_m(u)} + \frac{1}{w}\frac{K_m'(w)}{K_m(w)}\right]\omega\mu_0 G_1 = 0 \tag{1.74}$$

$$\left[\frac{\varepsilon_1}{u}\frac{J_m'(u)}{J_m(u)} + \frac{\varepsilon_2}{w}\frac{K_m'(w)}{K_m(w)}\right]\beta A_1 + \left(\frac{\varepsilon_1}{u^2} + \frac{\varepsilon_2}{w^2}\right)\omega\mu_0 m G_1 = 0 \tag{1.75}$$

where u and w are expressed with equations (1.43).
Finally, for hybrid modes HE and EH characteristic equation takes form [5, 7]

$$m^2\left(\frac{1}{u^2} + \frac{1}{w^2}\right)\left(\frac{1}{u^2} + \frac{s}{w^2}\right) = \left[Y_m(u) + X_m(w)\right]\left[Y_m(u) + sX_m(w)\right] \tag{1.76}$$

where $Y_m(u) = \frac{1}{u}\frac{J_m'(u)}{J_m(u)}$, $\quad X_m(w) = \frac{1}{w}\frac{K_m'(w)}{K_m(w)}$ (1.77)

and $s = \frac{\varepsilon_2}{\varepsilon_1}$ (1.78)

1.4.5. Type TE_{mp}, TM_{mp}, HE_{mp}, EH_{mp} Modes

So far we obtained the characteristic equations for three cases:

- TE type modes (45)

- TM type modes (51)
- EH and HE hybrid modes (1.76).

Solving the characteristic equations we can determine all components of electric and magnetic fields. Equations (1.52), (1.58) and (1.76) cannot be solved analytically, only graphically or numerically. Let us assume, that $s = \frac{\varepsilon_2}{\varepsilon_1} = \frac{n_2}{n_1} \approx 1$, because the difference of refractive indexes in real optical fiber is very little. This approximation is called weakly guiding approximation and means that modes propagate almost parallel to symmetry axis of optical fiber. In this case the characteristic equation (1.76) takes form

$$m^2\left(\frac{1}{u^2} + \frac{1}{w^2}\right)^2 = \left[Y_m(u) + X_m(w)\right]^2 \qquad (1.79)$$

or

$$\pm\, m^2\left(\frac{n_{ef}}{u^2 B}\right)^2 = \left[Y_m(u) + X_m(w)\right]^2 \qquad (1.80)$$

where

$$B = \frac{n_{ef}^2 - n_2^2}{n_1^2 - n_2^2} = \frac{w^2}{u^2 + w^2} = \frac{w^2}{\upsilon^2} \quad , \qquad 0 < B < 1 \qquad (1.81)$$

is named the normalized propagation constant, whereas

$$n_{ef} = \frac{\beta}{k_0} \qquad (1.82)$$

is called the effective refractive index. The effective refractive index is from the range between the refractive indices of the core and the cladding

$$n_2 \le n_{ef} \le n_1 \qquad (1.82.a)$$

Characteristic equation (1.80) (similarly as characteristic equations (1.52), (1.58) and (1.76), derived without weakly guiding approximation assumption) has several solutions for propagation constant β from equations (1.81-1.82) (that is for particular values of u and w, therefore for normalized frequency defined by equation (1.56)), for each integer value m indicating the order of Bessel function J_m and K_m. Let us mark the solutions with index m and arrange the solutions for consecutive values of propagation constant β from the smallest to the highest using index p.

Each eigenvalue of characteristic equation β_{mp} corresponds to a particular structure of electromagnetic field, which is called a **mode**. For each value of propagation constant β_{mp} the solutions for magnetic and electric fields can be obtained from equations (1.57) or (1.62)-(1.69). The intensities of magnetic and electric fields will be marked with two indexes m and p. Therefore we will obtain fields type TE_{op}, TM_{op} and HE_{mp}, EH_{mp}.

As we can see from the discussion thus far, propagation constant β is the key value in the electrodynamic analysis of modes propagating in optical fibers. Its physical meaning is the z component of wave vector $\beta = \frac{\omega}{\upsilon_f} = k_0 n_1 \sin\Theta$, z component is directed along the optical fiber axis, while Θ angle is the incident angle at core-cladding interface.

1.4.6. Cut-Off Frequency

The number of modes propagating in optical fiber depends on core diameter a, the index of refraction difference between core and cladding $n_1–n_2$ and the wavelength of wave propagating in optical fiber λ_0. We will prove, that the number of modes depends on previously derived (1.56) normalized frequency $\upsilon = \frac{2\pi a}{\lambda_0}\sqrt{n_1^2 - n_2^2}$.

Besides, we will show that the given mode can propagate in optical fiber only under condition that normalized frequency υ is higher than certain value, characteristic for each mode, named cut-off frequency. We will prove, that if υ<2.405 the characteristic equation has no solution, that is there exist no TE_{op} or TM_{op} type mode. The only mode propagating without limits is hybrid mode HE_{11}, which cut-off frequency is zero.

The optical fiber which propagates only one mode HE_{11}, called primary mode, is named single-mode fiber. As the value of υ increases, so does the number of solutions (modes). Therefore TE_{op} mode can propagate only when normalized frequency υ exceeds certain value υ_{op}, called cut-off frequency of TE_{op} mode. The optical fiber which propagates more than one mode is called multimode fiber. Fig. 1.23 shows the dependency of propagation constant B, expressed by equation (1.81) on normalized frequency υ. As it can be seen for υ<2.405 the only mode propagating without limits is a hybrid mode HE_{11}, which cut-off frequency is zero. For higher values of υ modes TE_{op} and TM_{op} as well as hybrid modes of higher order are propagated.

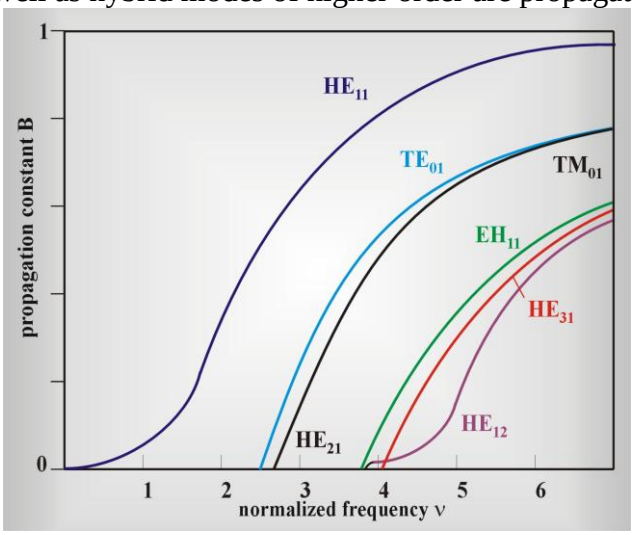

Fig. 1.23. The dependency of propagation constant B, expressed by equation (1.81) on normalized frequency υ, where B and v

Below we will show where does the condition of υ<2.405 arise from and state the term of cut-off frequency more precisely.

Characteristic equation (1.81) for modes EH and HE takes the form:

$$\pm m\left(\frac{1}{u^2} + \frac{1}{w^2}\right) = \left[\frac{1}{u}\frac{J_m'(u)}{J_m(u)} + \frac{1}{w}\frac{K_m'(w)}{K_m(w)}\right] \qquad (1.83)$$

Equation (1.52) takes the form

$$\frac{1}{u}\frac{J_0'(u)}{J_0(u)} = -\frac{1}{w}\frac{K_0'(w)}{K_0(w)} \tag{1.84}$$

Equation (1.58) takes the form

$$\frac{1}{u}\frac{J_0'(u)}{J_0(u)} = -\frac{1}{w}\frac{K_0'(w)}{K_0(w)} \tag{1.85}$$

if we introduce weakly guiding approximation assumption $s = \frac{\varepsilon_2}{\varepsilon_1} = \frac{n_2}{n_1} \approx 1$

Using the properties of the Bessel function

$$\pm uJ_m'(w) = mJ_m(w) \pm uJ_{m\pm1}(u) \tag{1.86}$$

$$\pm wK_m'(w) = mK_m(w) \pm wK_{m\pm1}(w) \tag{1.87}$$

$$J_{-m} = (-1)^m J_m \tag{1.88}$$

$$K_{-m} = KJ_m \tag{1.89}$$

it can be proved [8], that the characteristic equations take form

$$u\frac{J_{m-1}(u)}{J_m(u)} = -w\frac{K_{m-1}(w)}{K_m(w)} \tag{1.90}$$

When the mode cannot propagate in optical fiber, normalized propagation constant B=0 ((1.81) and Fig.1.23), that is when w=0, whilst normalized frequency (1.55)-(1.56) takes the value $\upsilon=u$ and has the physical meaning of mode **cut-off frequency** υ_{om}, that is the frequency above which particular mode can be propagated in optical fiber.

$$\upsilon_{om} = u \tag{1.91}$$

Because for w=0, $\frac{K_{m-1}(w)}{K_m(w)}$ takes a finite value, therefore (1.90) equals

$$u\frac{J_{m-1}(u)}{J_m(u)} = 0 \ . \tag{1.92}$$

As it arises from equation (1.92), in order to find cut-off frequency the roots of Bessel function must be found

$$J_{|m-1|}(u) = 0 \tag{1.93}$$

that is for *m=1* (*HE_{11}* mode) we look for the root of J_0 function which equals 2.405, as it can be seen in Fig. 1.15. We now understand why in the range of normalized frequencies

$$0 < \upsilon < 2.405 \tag{1.94}$$

only one mode is propagated - *HE_{11}*, which cut-off frequency equals zero. This kind of optical fiber is called single-mode. Only above the frequency υ_{om}=2.405 optical fiber becomes multimode. First it starts propagating *TE_{01}* and *HE_{21}* modes, and afterwards the modes with higher indexes (Fig. 1.23). The optical fiber becomes multimode. The number of modes propagated in optical fiber depends on its structure, expressed by equation (1.56)

$$\upsilon = \frac{\pi a}{\lambda_0}\sqrt{n_1^2 - n_2^2}$$

that is diameter *a*, wavelength of propagated wave λ_0 and refractive indexes of core n_1 and cladding n_2. If the cut-off frequency equals 2.405 for single-mode fibers, we

can calculate the wavelength of propagated wave. For typical single-mode fibers n_1-n_2=0.005, $a=5\ \mu m$ and we obtain $\lambda_0=?\ \mu m$, that is close infra-red range. In order for optical fiber to be able to propagate single mode from visible range (400-800 nm) it would have to have a very small core diameter $a<2\mu m$.

1.4.7. Linear Polarization Modes LP_{mp}

In reality single-mode fiber propagates two modes with orthogonal polarization. Mode HE_{11} consists of three components E_x , E_y, E_z and ether component E_x or E_y, dominates. Besides, linear combination of several modes of similar characteristic properties produces the resultant electric field, linearly polarized, of negligible component in the light propagation direction in fiber $E_z=0$. This kind of modes is called linearly polarized L_{mp}. It can be proved [7], that

$$\begin{aligned} LP_{0p} &= HE_{1p} \\ LP_{1p} &= HE_{2p} + E_{0p} + H_{0p} \\ LP_{mp} &= HE_{m+1,p} + EH_{m-1,p} \qquad m>2 \end{aligned} \tag{1.95}$$

Two modes with orthogonal polarization are degenerated, i.e. characteristic equation has two solutions, corresponding to the same propagation constant β defined by equation (1.19) and connected with effective refractive index by formula (1.82). Degeneration corresponds to ideal conditions with no birefringence. In reality stresses, density changes, random changes of core shape and diameter, cause the formation of discriminated optical axes, therefore birefringence phenomenon. In consequence two orthogonal components travel in optical fiber as ordinary and extraordinary beams propagating with different speeds. In consequence the degeneration of two modes with orthogonal polarization is eliminated. Different speeds of two orthogonal components generate phase difference changing during propagation along fiber and random mixing the two components which causes polarization change. As we mentioned in Chapter 3 there are optical fibers which preserve linear polarization along one of the fiber principal axes.

We will show after [5, 7] that hybrid mode indeed consists of two components with mutually perpendicular polarization. In weakly guiding approximation assumption, that is when

$$s = \frac{\varepsilon_2}{\varepsilon_1} = \frac{n_2}{n_1} \approx 1 \tag{1.96}$$

we proved that characteristic equation for hybrid modes HE and EH takes form (1.80)

$$m\left(\frac{1}{u^2} + \frac{1}{w^2}\right) = \pm\left[Y_m(u) + X_m(w)\right] \tag{1.97}$$

and the propagation constant β is given by formula

$$\beta = \omega\sqrt{\varepsilon\mu_0} \tag{1.98}$$

Substituting equations (1.95) and (1.98) to (1.74) we obtain the correlation between constants A_1 and G_1.

$$G_1 = \pm\sqrt{\frac{\varepsilon}{\mu_0}}A_1 \tag{1.99}$$

where + sign corresponds to HE modes, while – sign corresponds to EH modes.

Substituting equation (1.99) to (1.62) and (1.64) we obtain the components along optical fiber axis *z*

$$\tilde{E}_z = A_1 J_m(h_1 r)\cos m\phi \tag{1.100}$$

$$H_z = \pm A_1\sqrt{\frac{\varepsilon}{\mu_0}}\, J_m(h_1 r)\sin m\phi \tag{1.101}$$

Following the analogous procedure for F_1 and B_1 constants in (1.61) for orthogonal solution we obtain

$$F_1 = \pm\sqrt{\frac{\varepsilon}{\mu_0}}\, B_1 \tag{1.102}$$

where + sign corresponds to HE modes, while – sign corresponds to EH modes and components along *z* axis from equations (1.27) and (1.31)

$$\tilde{E}_z = B_1 J_m(h_1 r)\sin m\phi \tag{1.103}$$

$$H_z = {}^{+}_{-} B_1\sqrt{\frac{\varepsilon}{\mu_0}}\, J_m(h_1 r)\cos m\phi \tag{1.104}$$

because A_1 and G_1 =0 for this case.

Transverse components *x* and *y* of the field we can calculate from Maxwell equations in Cartesian coordinate system, not in spherical coordinate system, which we have used thus far.

$$\tilde{E}_x = -\frac{1}{h^2}\left(\gamma\frac{\partial\tilde{E}_z}{\partial x} + i\omega\mu\frac{\partial\tilde{H}_z}{\partial y}\right) \tag{1.105}$$

$$\tilde{E}_y = \frac{1}{h^2}\left(-\gamma\frac{\partial\tilde{E}_z}{\partial y} + i\omega\mu\frac{\partial\tilde{H}_z}{\partial x}\right) \tag{1.106}$$

$$\tilde{H}_x = \frac{1}{h^2}\left(i\omega\varepsilon\frac{\partial\tilde{E}_z}{\partial y} - \gamma\frac{\partial\tilde{H}_z}{\partial x}\right) \tag{1.107}$$

$$\tilde{H}_y = -\frac{1}{h^2}\left(i\omega\varepsilon\frac{\partial\tilde{E}_z}{\partial x} + \gamma\frac{\partial\tilde{H}_z}{\partial y}\right) \tag{1.108}$$

Because field components (1.86) and (1.87) are expresses in spherical coordinates, in equations (1.105)-(1.108) the exchange of coordinates have to be performed, using the correlation

$$\frac{\partial r}{\partial x} = \cos\phi\,, \qquad \frac{\partial r}{\partial y} = \sin\phi$$

$$\frac{\partial\phi}{\partial x} = -\frac{1}{r}\sin\phi\,, \qquad \frac{\partial\phi}{\partial y} = \frac{1}{r}\cos\phi \tag{1.109}$$

and using Bessel function properties

$$uJ_m'(u) = +mJ_m(u) - uJ_{m+1}(u)$$

$$uJ_m'(u) = -mJ_m(u) + uJ_{m-1}(u) \tag{1.110}$$

In order to obtain components of linearly polarized modes L_{mp} several modes of similar characteristic properties must be combined so that obtained resultant electric field is characterized by negligible components in light propagation direction $\tilde{E}_z = 0$ and $\tilde{H}_z = 0$. This condition is met for combination described by equations (1.95).

Substituting equations (1.100)-(1.109) to (1.95) we obtain four electromagnetic field components for four linearly polarized modes L_{mp}
We get the modes with polarization in *x* direction

$$\tilde{\tilde{E}}_x = \tilde{\tilde{H}}_y Z_1 = E_m \frac{J_m(ur/a)}{J_m(u)} \cos m\phi \qquad r<a \qquad (1.111)$$

$$\tilde{\tilde{E}}_x = \tilde{\tilde{H}}_y Z_2 = \tilde{\tilde{E}}_m \frac{K_m(wr/a)}{K_m(w)} \cos m\phi \qquad r>a$$

$$\tilde{\tilde{E}}_y = 0, \qquad \tilde{\tilde{H}}_x = 0$$

$$\tilde{\tilde{E}}_x = \tilde{\tilde{H}}_y Z_1 = \tilde{\tilde{E}}_m \frac{J_m(ur/a)}{J_m(u)} \sin m\phi \qquad r<a \qquad (1.112)$$

$$\tilde{\tilde{E}}_x = \tilde{\tilde{H}}_y Z_2 = \tilde{\tilde{E}}_m \frac{K_m(wr/a)}{K_m(w)} \sin m\phi \qquad r>a$$

$$\tilde{\tilde{E}}_y = 0, \qquad \tilde{\tilde{H}}_x = 0$$

and the modes with polarization in *y* direction

$$\tilde{\tilde{E}}_y = -\tilde{\tilde{H}}_x Z_1 = \tilde{\tilde{E}}_m \frac{J_m(ur/a)}{J_m(u)} \cos m\phi \qquad r<a \qquad (1.113)$$

$$\tilde{\tilde{E}}_y = -\tilde{\tilde{H}}_y Z_2 = \tilde{\tilde{E}}_m \frac{K_m(wrIa)}{K_m(w)} \cos m\phi \qquad r>a$$

$$\tilde{\tilde{E}}_x = 0, \qquad \tilde{\tilde{H}}_y = 0$$

where

$$Z_1 = \sqrt{\frac{\mu_0}{\varepsilon_1}}, \qquad Z_2 = \sqrt{\frac{\mu_0}{\varepsilon_2}} \qquad (1.114)$$

while E_m denotes maximum value of electromagnetic field intensity at the core-cladding interface. It arises from equations (1.111)-(1.113) that for *m=0* only two non-zero modes L_{0p} exist.
The components can be calculated from Maxwell equations and it can be proved, that components in propagation direction *z* are negligible as compared to transverse components *x* and *y*.

$$\tilde{\tilde{E}}_z = \frac{i}{\omega\varepsilon}\left(\frac{\partial\tilde{\tilde{H}}_z}{\partial y} - \frac{\partial\tilde{\tilde{H}}_y}{\partial x}\right) \qquad (1.115)$$

$$\tilde{\tilde{H}}_z = \frac{i}{\omega\mu_0}\left(\frac{\partial\tilde{\tilde{E}}_y}{\partial x} - \frac{\partial\tilde{\tilde{E}}_x}{\partial y}\right) \qquad (1.116)$$

Fig. 1.24 presents transverse intensity distribution for several initial linearly polarized modes. For L_{0p} two identical mutually orthogonal components exist. For higher indexes four modes exist, which differ not only in polarization, but in intensity distribution orientation as well.

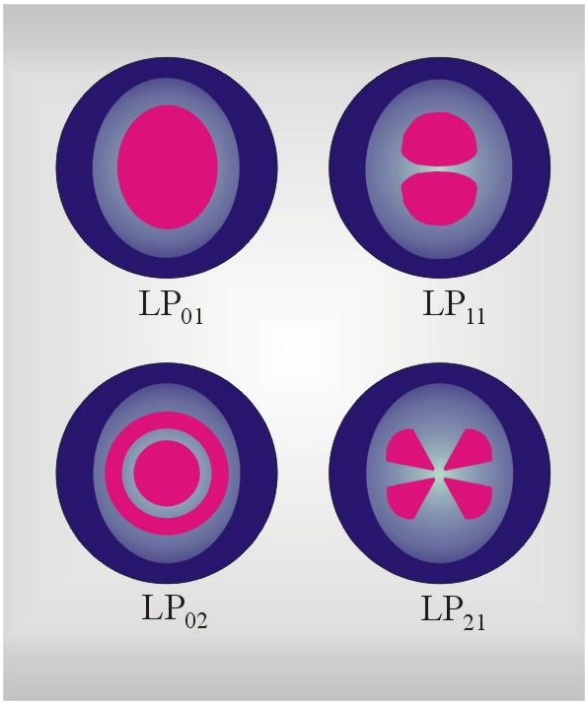

Fig. 1.24 Intensity distribution in cylindrical optical step-index fiber core for linearly polarized modes.

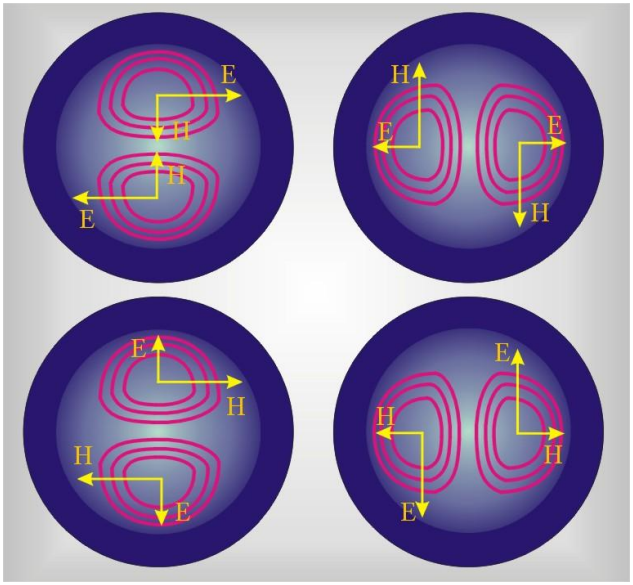

Fig. 1.24 Intensity and orientation field distribution in cylindrical optical step-index fiber core for linearly polarized LP_{11} mode.

1.5. Propagation Of Light In Optical Fibers. Electrodynamic Analysis. Planar Optical Waveguide. Graphical Solution Of Characteristic Equation.

Thus far we only analyzed the modes in cylindrical step-index fiber. Because of the fiber geometry we used spherical coordinates. The solutions for Maxwell equations are Bessel functions, while continuity conditions and conditions arising from symmetry allow to obtain characteristic equation for propagation constant β. This parameter is a key quantity in electrodynamic analysis of modes propagating in optical fibers. It has physical meaning of wave vector $\beta = \frac{\omega}{\upsilon_f} = k_0 n_1 \sin\Theta$, z component is directed along fiber axis, while Θ is the incident angle at core-cladding interface.

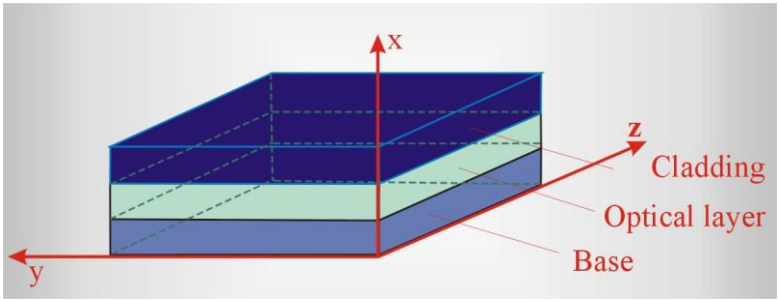

Fig.1.26. Planar waveguide.

In coordinates system applied in calculations x axis is perpendicular to base and coating interface $-\frac{h_0}{2} < x < \frac{h_0}{2}$, where h_0 is the thickness of core layer of planar waveguide, light propagates along z axis. For calculation simplification we assume that the dimension of waveguide in y axis direction is indefinite. We also make the assumption that planar waveguide is symmetric (refractive indexes of base n_2 and coating are identical $n_3 = n_2$). Core refractive index n_1 is higher from both n_2 and n_3.
The solution of Maxwell equations for planar waveguide presented in Fig. 1.8. is much simpler [6]. Below we will discuss Maxwell equations for TE type modes. In light of the above made assumptions, wave field is restricted only in x direction, therefore y derivatives equal zero, than

$$\tilde{H}_y = \tilde{E}_x = \tilde{E}_z = 0 \qquad (1.117)$$

$$\frac{\partial^2 \tilde{E}_y}{\partial x^2} + h^2 \tilde{E}_y = 0 \qquad (1.118)$$

$$h^2 = \gamma^2 + n^2 k_0^2 \text{ , where } \gamma = \alpha + i\beta \qquad (1.119)$$

β denotes phase constant and is named propagation constant, while α describes attenuation (and decay of oscillating wave) in waveguide. The solution of equation (1.118) should have oscillating characteristics in core and decay in coating. In order for this condition to he met, h has to be real in the core and imaginary in coating, thus

$$h = h_1 \text{ for core } |x| < \frac{h_0}{2}. \text{ and } \quad h = ih_2 \text{ for coating } |x| > \frac{h_0}{2} \qquad (1.120)$$

$$\frac{\partial^2 \tilde{E}_y}{\partial x^2} + h_1^2 \tilde{E}_y = 0 \text{ for core } |x| < \frac{h_0}{2} \qquad (1.121)$$

$$\frac{\partial^2 \tilde{E}_y}{\partial x^2} + h_2^2 \tilde{E}_y = 0 \text{ for coating } |x| > \frac{h_0}{2} \qquad (1.122)$$

Because attenuation in waveguide is low, we can assume with good approximation α=0, therefore the equations (1.121) and (1.122) take form

$$\frac{\partial^2 \tilde{E}_y}{\partial x^2} + \left(n_1^2 k_0^2 - \beta^2\right)\tilde{E}_y = 0 \text{. for core } |x| < \frac{h_0}{2} \tag{1.123}$$

$$\frac{\partial^2 \tilde{E}_y}{\partial x^2} - \left(\beta^2 - n_2^2 k_0^2\right)\tilde{E}_y = 0 \qquad \text{for coating } |x| > \frac{h_0}{2} \tag{1.124}$$

$$\text{where } h_1^2 = \beta^2 - n_1^2 k_0^2 < 0 \text{ for core } |x| < \frac{h_0}{2} \tag{1.125}$$

$$h_2^2 = \beta^2 - n_2^2 k_0^2 > 0 \text{ for coating } |x| > \frac{h_0}{2} \tag{1.126}$$

because

$$k_0^2 n_2^2 < \beta^2 < k_0^2 n_1^2 \tag{1.127}$$

The solution of equation (1.123) in core is oscillating wave

$$\tilde{E}_y(x) = a \cos \kappa x \text{ for core } |x| < \frac{h_0}{2} \tag{1.128}$$

where *a* is integration constant
while outside core the solution of equation (1.124) is attenuating wave

$$\tilde{E}_y(x) = ce^{-\gamma x} \text{ for coating } |x| > \frac{h_0}{2} \tag{1.129}$$

From the condition of continuity for $\tilde{E}_y(x)$ and derivative $\frac{d\tilde{E}_y}{dx}$ at the core-cladding (base or coating) interface for $x = \pm \frac{h_0}{2}$ we obtain

$$a \cos\left(\frac{h_2 h_0}{2}\right) = c \exp(-\gamma h_0 / 2) \tag{1.130}$$

$$-\kappa a \sin\left(\frac{h_0 h}{2}\right) = -\gamma c \exp(-\gamma h_0 / 2) \tag{1.131}$$

Dividing bilaterally the equations (1.130) and (1.131) and multiplying both sides by $\frac{h_0}{2}$ we obtain

$$\frac{h_2 h_0}{2} tg\left(\frac{h_2 h_0}{2}\right) = \frac{h_0}{2} h_1 \tag{1.132}$$

From equations (1.125) and (1.126) we get

$$(h_1^2 + h_2^2) = k_0^2\left(n_1^2 - n_2^2\right) \tag{1.133}$$

Let us introduce the term of normalized frequency, similarly as for cylindrical fiber equations ((1.55)-(1.56.a)), by multiplying both sides of equation (1.133) by $\frac{h_0}{2}$

$$\upsilon = \frac{h_0}{2}\sqrt{(h_1^2 + h_2^2)} = k_0 \frac{h_0}{2}\sqrt{\left(n_1^2 - n_2^2\right)} \tag{1.134}$$

From the introduced normalized frequency υ we can next write

$$\frac{h_1 h_0}{2} = \left(\frac{\upsilon^2}{4} - \xi^2 \right)^{\frac{1}{2}} \quad , \quad \text{where} \quad \xi = \frac{h_2 h_0}{2} \tag{1.135}$$

Therefore, equation (1.132) can be expressed using normalized frequency υ as below

$$\xi tg\xi = \left(\frac{\upsilon^2}{4} - \xi^2 \right)^{\frac{1}{2}} \tag{1.136}$$

or

$$\xi tg\xi = \left(\upsilon_0^2 - \xi^2 \right)^{\frac{1}{2}} \tag{1.137}$$

where

$$\upsilon_0 = \frac{\upsilon}{2} \tag{1.138}$$

The right side of equation (1.137)

$$\eta = \left(\upsilon_o^2 - \xi^2 \right)^{\frac{1}{2}} \tag{1.139}$$

describes a circle of υ_0 diameter on *(η, ξ)* plane.

Equation (1.137) serves as characteristic equation, as it allows to calculate propagation constant *β*. Equation (1.137) can be solved graphically. Intersection point of a circle of υ_0 diameter described by equation (1.139) and $\xi tg\xi$ function from equation (1.137) allows to calculate propagation constant.

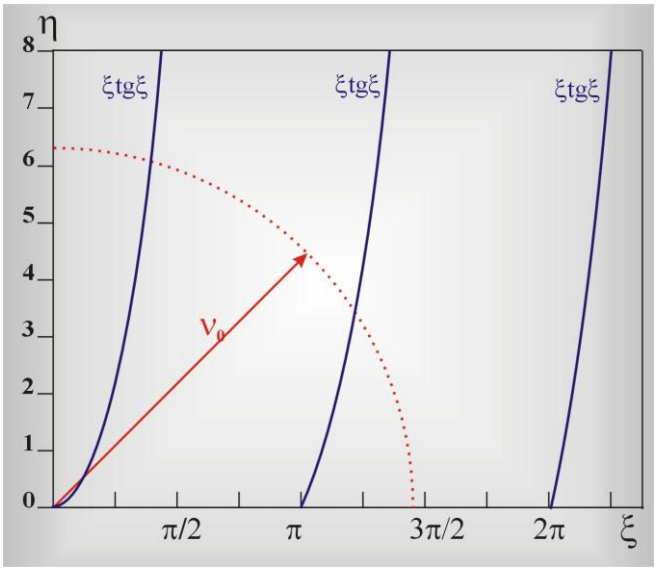

Fig. 1.27. Graphic illustration of solution of planar symmetrical waveguide equation. Point of intersection of a circle described by equation (1.139) and $\xi tg\xi$ function from equation (1.137) allows for determination of propagation constant.

Normalized frequency from equation (1.134) has the physical sense of cut-off frequency υ_{om}, that is the frequency, below which light cannot propagate in waveguide core, when h_2 in formula (1.133) equals zero, which arises from equation (1.126), as β cannot be lower than $n_2^2 k_0^2$. In this case $\xi = \upsilon_0$. From the graphical solution presented in Fig. 1.27. it arises that for frequencies υ_o satisfying the condition

$$0 < \upsilon_0 < \frac{\pi}{2} \qquad (1.140)$$

only one TE mode exists and therefore planar waveguide is single-mode. For higher υ_0 values planar waveguide becomes multimode.

For planar waveguide it is very easy to derive the dependency between propagation constant B expressed by formula (1.81) on normalized frequency υ presented in Fig.1.23. Using the formula for normalized propagation constant B from equation (1.81) and notation which we introduced for planar waveguide (1.135) and (1.138)

$$B = \frac{n_{ef}^2 - n_2^2}{n_1^2 - n_2^2} = \frac{h_1^2}{h_1^2 + h_2^2} = \frac{h_1^2}{\upsilon^2} = 1 - \frac{h_2^2}{\upsilon^2} \quad , \qquad 0 < B < 1 \quad (1.141)$$

where

$$n_{ef} = \frac{\beta}{k_0}$$

we obtain

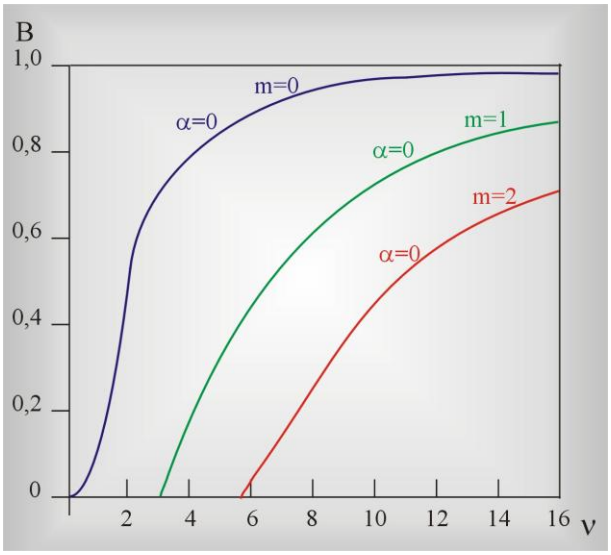

Fig. 1.28. Dependency of normalized propagation constant B on normalized frequency υ for planar symmetrical waveguide calculated from equation (1.145)

$$tg^2\left(\upsilon_0\sqrt{1-B}\right) = \frac{B}{1-B} \qquad (1.142)$$

or more generally (as $tg\alpha = tg(\alpha + m\pi)$)

$$tg\left(\upsilon_0\sqrt{1-B} + \frac{m\pi}{2}\right) = \pm\sqrt{\frac{B}{1-B}} \qquad (1.143)$$

that is

$$\upsilon_0 = \sqrt{\frac{1}{1-B}}\left[\frac{m\pi}{2} + arctg\sqrt{\frac{B}{1-B}}\right], \qquad \text{m=0,2,4,6,..} \qquad (1.145)$$

This is the dependency of normalized propagation constant B on normalized frequency υ for planar symmetrical waveguide.

1.6. Propagation Of Light In Optical Fibers. Analysis Of Optical Path And Electrodynamic Analysis For Gradient-Index Cylindrical Fiber [6]

In gradient-index fiber the profile of core refractive index is not constant and depends on distance r from central axis. Most often this kind of optical fibers is characterized by profile in which core refractive index is described by the equation

$$n(r) = n_0 - \frac{1}{2} n_r r^2 \qquad (1.146)$$

and is a function of distance r from fiber axis and $n_0 >> n_r$.

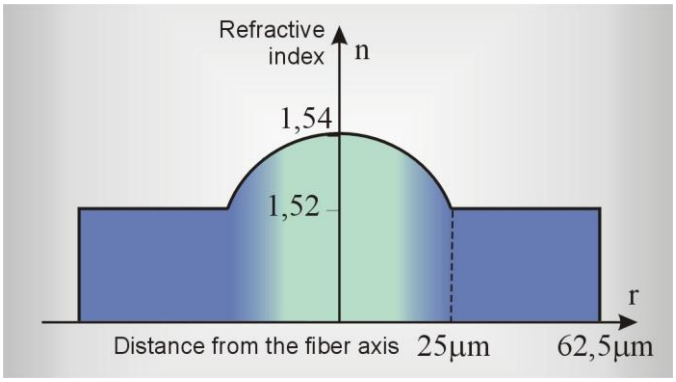

Fig. 1.29. Refractive index profile in gradient-index fiber.

Therefore the assumption which we used in chapter 4.1., that refractive index $n(\omega)$ is independent from spatial components of core and cladding, is not valid for gradient-index fibers.
First of all, we would like to understand why the tracks of beams in gradient-index fiber are sinusoidal or helical, like in the Figure below.

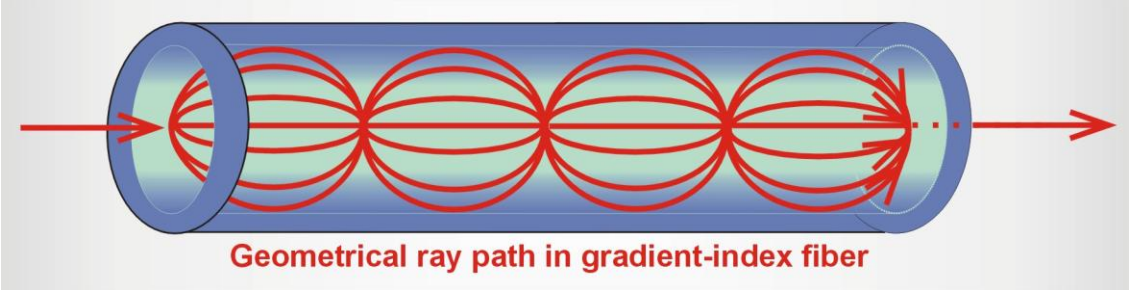

Fig.1.30. Beam trajectories in gradient-index fiber.

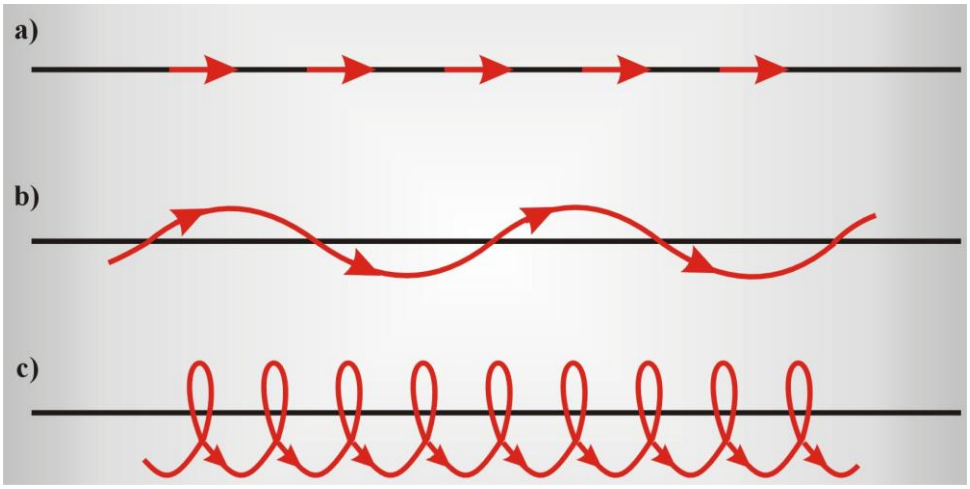

Fig. 1.31 *Beam trajectories in gradient-index fiber*

Using Fermat's principle

$$\frac{\partial^2 r}{\partial z^2}\,\vec{\rho} = \frac{1}{n(r)}\,\nabla n(r) \tag{1.147}$$

$$\vec{r} = x\vec{r} + y\vec{j}\ ,$$

$$\nabla n(r) = -n_r x\vec{i} - n_r y\vec{j} \tag{1.148}$$

$$\frac{\partial^2 r}{\partial z^2}\,\vec{\rho} = \frac{-n_r x\vec{i} - n_r y\vec{j}}{n_0 - \frac{1}{2}\,n_r(x^2 + y^2)} \tag{1.149}$$

or, after conversion

$$\left[\frac{\partial^2 r}{\partial z^2} - \frac{1}{2}\,\frac{n_r}{n_0}\left(x^2 + y^2\right)\frac{\partial^2 r}{\partial z^2}\right]\vec{\rho} + \frac{n_r}{n_0}\,x\vec{i} + \frac{n_r}{n_0}\,y\vec{j} = 0 \tag{1.150}$$

because

$n_r << n_0$, and $r^2 = x^2 + y^2$ - is negligible therefore:

$$\frac{\partial^2 r}{\partial z^2}\,\vec{\rho} + \frac{n_r}{n_0}\,\vec{r} = 0$$

$$\frac{\partial^2 r}{\partial z^2} + \frac{n_r}{n_0}\,r = 0 \tag{1.151}$$

we obtain the equation describing radiation pathway in gradient-index fibers (parabolic)

$$r(z) = r_0\left[\cos\left(\sqrt{\frac{n_r}{n_0}}\,z\right)\right] + r_0'\left[\sqrt{\frac{n_0}{n_r}}\,\sin\left(\sqrt{\frac{n_r}{n_0}}\,z\right)\right] \tag{1.152}$$

which actually has the character of harmonic function, as presented in Fig. 1.30.

Secondly, we are interested in finding the cross-section of electromagnetic fields for gradient-index fibers. We follow the similar procedure as described in Chapters 4.1 and 5, that is we use Helmholtz equation in form

$$\frac{\partial^2 \tilde{E}}{\partial x^2} + \frac{\partial^2 \tilde{E}}{\partial y^2} + \left[k_0^2 n^2(r) - \beta^2\right]\tilde{E} = 0 \qquad (1.153)$$

where

$$\tilde{E}(x, y, z, t) = \tilde{E}(x, y)\, exp\left[i(\omega t) - \beta z\right] \qquad (1.154)$$

and refractive index is described by function

$$n(r) = n_0 - \frac{1}{2} n_r r^2 \approx n_1^2 (1 - \frac{r^2}{G^2}) \qquad (1.155)$$

where $G^{-1} = \frac{\sqrt{2\Delta n}}{a}$, $\Delta n = n_1 - n_2$, and *a* is core diameter.

Substituting (1.155) to (1.153), applying field coordinates separation in the plane perpendicular to fiber axis *z*

$$\tilde{E}(x, y) = X(x)Y(y) \qquad (1.156)$$

we obtain equations for $X(x)$ and $Y(y)$ components, which solution are **Hermite-Gauss functions** H_m and H_p. Finally we obtain the description of field intensity in form

$$\tilde{E}(x, y, z) = E_0 H_m\left(\frac{\sqrt{2x}}{w}\right) H_p\left(\frac{\sqrt{2y}}{w}\right) exp\left(-\frac{r^2}{w^2}\right) exp\left[-ik(1-\beta)^{\frac{1}{2}} z\right] \qquad (1.157)$$

where: $w^2 = \frac{2G}{k}$

For *m=0 i p=0* Hermite functions $H_m = H_p = 1$**,** which means that basic mode is characterized by transverse Gaussian distribution in gradient-index fiber.

1.7. Production of glass fibers

Crucial factor in production of optical fibers with long distance transmission ability is technique of production, modification and control the following fiber parameters:

- Attenuation
- Non-linearity
- Dispersion
- Refractive index
- Core doping with rare earths elements atoms.

Optical fibers are produced from different materials:

- Glass optical fibers from pure quartz and silica SiO_2 (which also can be doped), core diameter 5-10 μm (SMF), 50/62.5 μm (MMF), transmission for distances of kilometers. For telecommunications only this type of material is used;
- Fluoride glass fibers, among which the one of greatest importance is type ZBLAN glass (ZrF, BaF_2, LaF_3, AlF_3, NaF in proportion 53:20:4:3:20)
- Fluoride glass fibers (KCl, TlBrI),

- Plastic optical fibers APF (both core and cladding are made of PMMA), core diameter 980/1000 μm, 650 nm, attenuation is about 220 dB/km, maximum transmission distance of the order of 50 m.
- Plastic optical fibers PCF (core is made of glass, cladding made of plastic), core diameter 200/300 μm, 800 nm, attenuation – c.a. 6 dB/km, maximum transmission distance – up to 1km,
- Semiconductor optical fibers made of epitaxial layers (e.g. GaAs/AlGaAs)
- Dielectric layers (Ta_2O_5, ZnO, Si_3N_3/SiO_2).

Most commonly used optical fibers are made of pure silica glass (SiO_2). Cladding is made of glass, while core glass is admixed with proper amount of dopants – usually germanium or lead are admixed – which increase the index of refraction of core as compared to that of cladding.

Fig. 1.32. presents typical method for optical fibers production. It belongs to the group of Chemical Vapour Deposition (CVD) methods and consists in deposition of silicon dioxide doped with other oxides in vapour phase. This method allows for deposition of numerous layers of different refractive indexes in order to obtain gradient-index fiber. In optical fiber production using this method the rotating silica substrate tube of c.a. 15 mm in diameter and 1 m length is subjected to an internal flow of material in gaseous phase. The tube constitutes cladding material and blown-in material creates the core. Core material is the mixture of silicon chloride ($SiCl_4$) and admixture elements chlorides (e.g. germanium $GeCl_4$). The deposition is accomplished by an external, local application of high temperature of the order of 1200-1400 ^{0}C. In such temperature chlorides react with oxygen from carrier gas

$$SiCl_4 + O_2 \rightarrow SiO_2 + 2Cl_2$$

$$GeCl_4 + O_2 \rightarrow GeO_2 + 2Cl_2$$

Resulting from the above reactions silica (SiO_2) powder and germanium oxide deposit on the inner surface of the quartz tube. The obtained powder is sintered into a thin layer of about 10 μm. Refractive indexes are controlled by application of adequate admixtures. The admixture of B_2O_3 and F_2 causes decrease in glass index value, while admixture of GeO_2, P_2O_5, Al_2O_3 causes increase in glass index value.

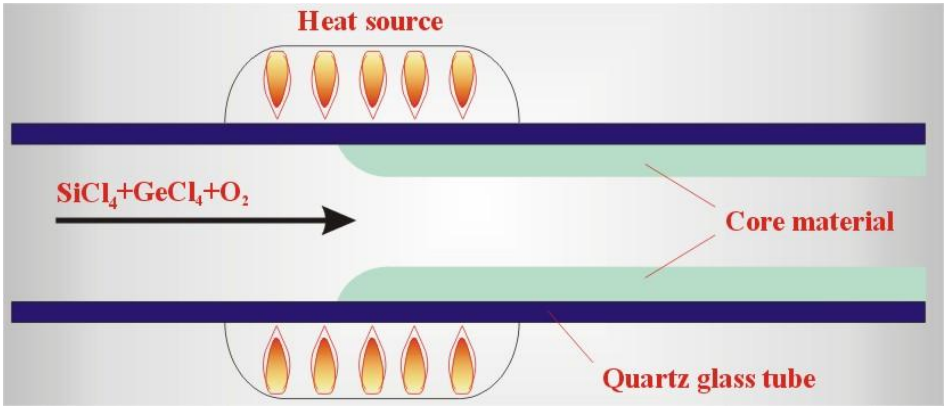

Fig.1.32. Diagram illustrating CVD method

After the deposition process is finished the temperature in raised to the melting point. Applied temperature depends on the kind of glass, pure quartz glasses are characterized by high melting points (2000 ^{0}C), however, the admixture of sodium or calcium oxide lower melting temperature to 1400 ^{0}C. In melting temperature the outer tube softens, begins to melt and contract. This process, called collapse, leads to formation of perform, which is next drawn into fibers in the plastic heat treatment process. The quality of perform depends on collapse speed and homogeneity, which is dependant on uniformity of rotation during heating and oxygen pressure inside the tube. The parameters influencing perform quality depend on silica deposition method on quartz cladding. CVD method was improved for fiber optics applications by Modified Chemical Vapor Deposition MCVD method (Fig. 1.33.), Plasma Chemical Vapor Deposition (PCVD), Plasma Modified Chemical Vapor Deposition (PMCVD), Outside Vapor Deposition (OVD) and Vapor Axial Deposition (VAD).
CVD, MCVD, PCVD and PMCVD methods are similar in their main idea, however they differ in the speed of glass creation, which is known to influence its isotropy and lack of distinguished optical axes arising from local stresses.
PCVD method is shown in Fig. 1.34. In this method, the speed of glass deposition is higher than in CVD method, due to application of plasma of temperature 1200^{0}C produced in microwave oven (2.5 GHz) which travels along the tube with the speed of several meters per minute, substituting the torch. This method is applied in telecommunication optical fibers. In PMCVD method plasma reaches the temperature close to 9000 ^{0}C, which substantially increases deposition speed of silica glass.

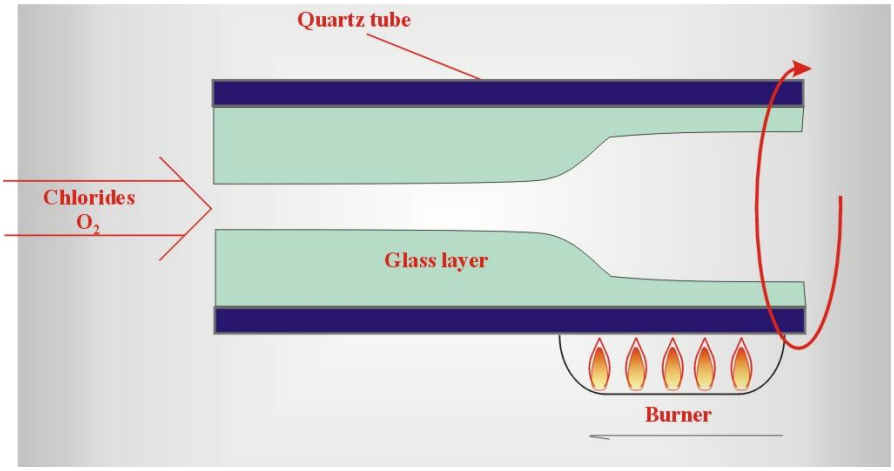

Fig.1.33. Diagram illustrating MCVD method

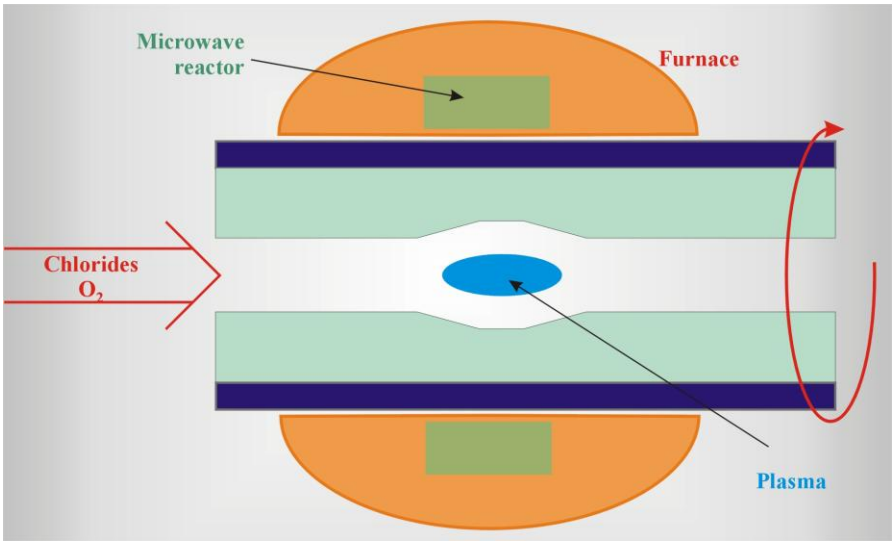

Fig.1.34. Diagram illustrating PCVD method

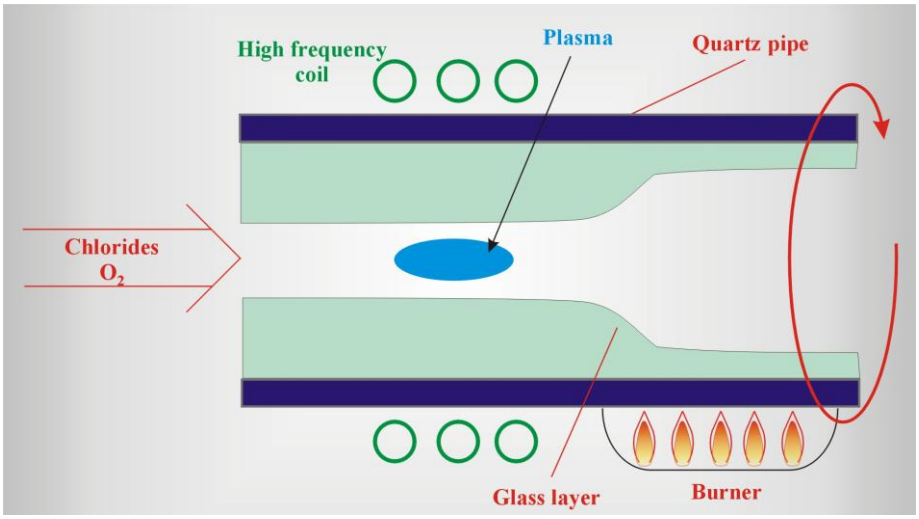

Fig.1.35. Diagram illustrating PMCVD method

The process of perform generation in OVD method is basing on different principal. The products of low energy reaction between silicon (and admixtures) chlorides and oxygen deposit on graphite rod, which is subsequently removed due to different thermal expansion coefficients of the rod and silica. The obtained silica glass tube is sufficient for drawing a fiber of 30-40 km length.

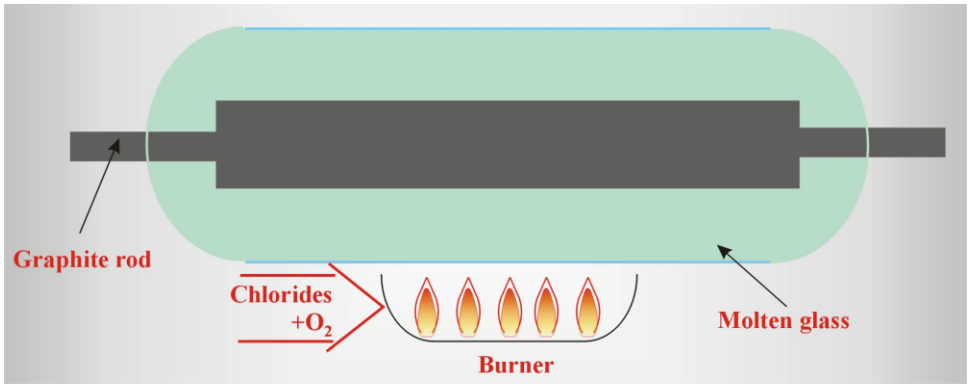

Fig.1.36. Diagram illustrating OVD method

Preform is subsequently used for production of the fiber. The diagram of fiber fabrication system is presented in Fig. 1.37.

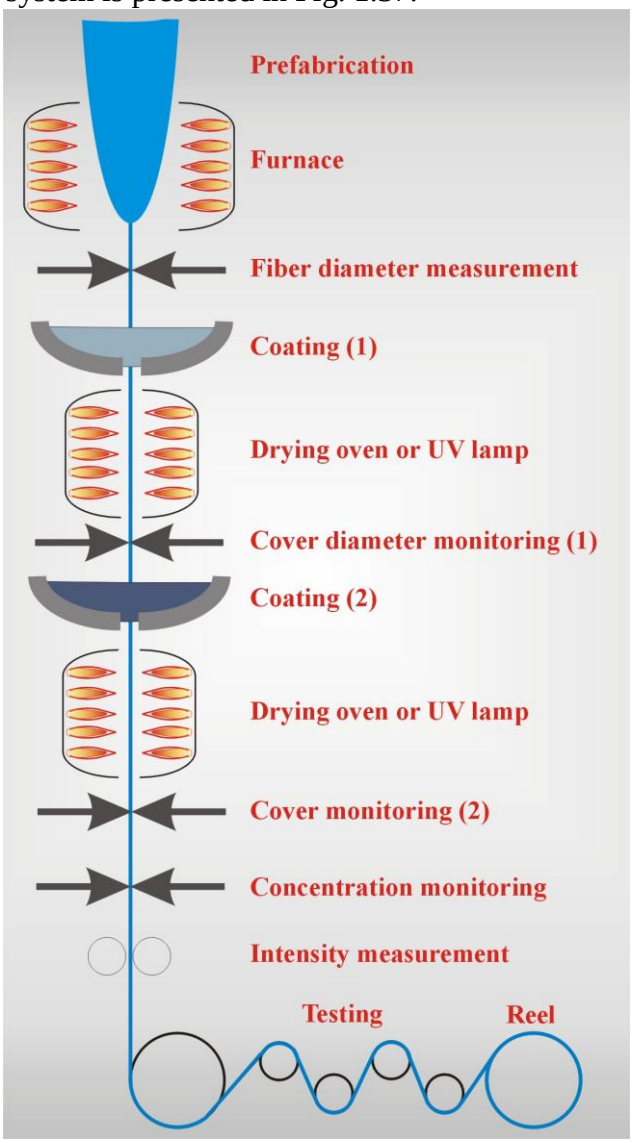

Fig.1.37. Diagram of fiber fabrication system

Other methods of optical fiber drawing include:

- **double crucible method** in which the core and cladding melts are formed separate crucibles and combined in the drawing process (Fig.). This method can be used for step-index fibers production, as well as gradient-index fibers. Gradient-index fibers are obtained by ion exchange between different kinds of glasses in the process of diffusion. This method is less commonly used and is applied for drawing fibers no longer than 10 km.
- "rod-in-tube" method, in which the core and cladding are cast separately, positioned concentrically, than heated up to glass softening temperature and drawn into thin threads.

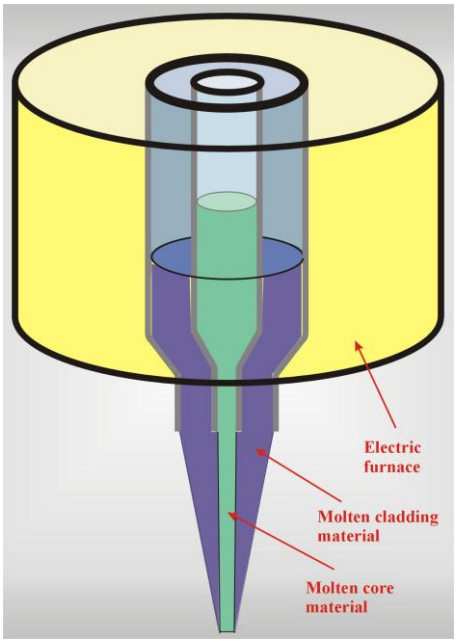

Fig.1.38. Diagram of double crucible system

Separate group of optical fibers constitute polarization maintaining fibers, already mentioned in Chapter 3. In some applications maintaining constant polarization in optical fiber is crucial, e.g. fiber optics interferometers, fiber optics lasers, sensors, optoelectric modulators, coherent transmission and integrated optical circuits coupling. Moreover, in all optical fibers, in lower or higher extent, attenuation depends on polarization and impedes signal transmission in optical fiber. In polarization maintaining fibers HB (high birefringence) type birefringence must be produced by design. In this case random polarization changes resulting from density fluctuations and temporary stress axes become negligible, as they are masked by controlled, deliberately introduced birefringence. If we align light polarization and distinguished optical axis of fiber it will not change during propagation along the fiber. We distinguish internal and induced birefringence. Internal birefringence is achieved in fiber production process, by shaping the perform in order to obtain the core of adequate shape or suitable refractive index profile. Usually it means elliptical core shape (Fig. 1.39) or elliptical refractive index profile. This kind of optical fibers is called low birefringence (LB).

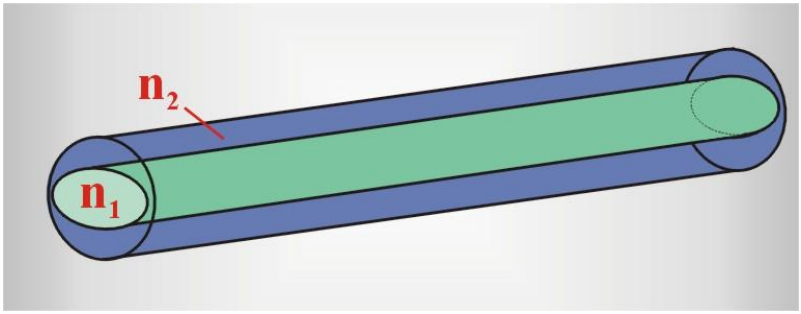

Fig.1.39. Optical fiber maintaining polarization by elliptical core form.

Another method of birefringence induction in fiber is creating internal stresses. Fig. shows the structure of most common fibers which maintain polarization by internal stresses creation. As we can notice in Panda type fiber cross-section, next to the core there are two additional orifices if cladding which are filled with rods made

of material of higher thermal expansion coefficient than cladding (usually borosilicate glass). In fiber drawing process stresses arise along the fiber distinguished axis, which produce controlled birefringence. This also causes that the fiber acts as polarization analyzer and transmits only the light in one polarization plane. Different solutions are presented in Fig. . For example, in D type fiber, cladding is beveled in the manner that the plane is parallel to optical axis of the fiber. In elliptical fibers, core cross-section is shaped as an ellipse. [R.B. Dyott, Elliptical Fiber Waveguides, Artec House, Boston, 1995]

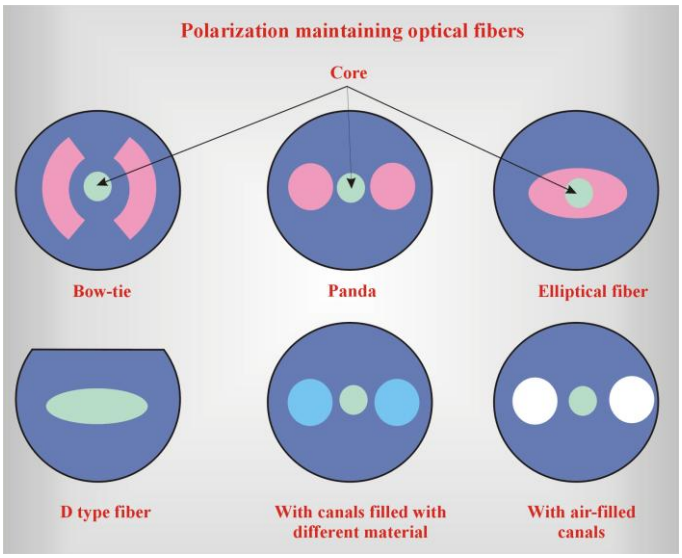

Fig.1.40. Structure of polarization maintaining optical fibers.

1.8. Waveguides Optical Windows

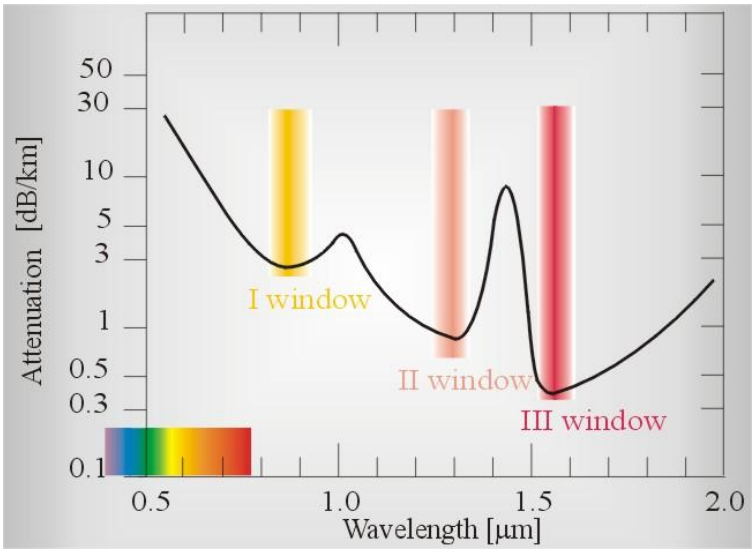

Fig .1.41. Attenuation dependence on wavelength.

Table 1.1. Optical windows.

Optical window	Wavelength [nm]	Attenuation [dB/km]
I	850	~3
II	1300	0,3 – 0,5

III	1550	0,18 – 0,3

Optical signal propagating in optical fiber is a subject to attenuation. First optical fibers were characterized by so high attenuation, that their wide use was not projected, especially it seemed impossible to apply them for long distance transmissions. In 1972 American company Corning Glass first introduced multimode optical fiber with attenuation of 4 dB/km for wavelength 850 nm.
Attenuation has different causes, the most important of which are:

- Rayleigh scattering ($T \propto \frac{1}{\lambda^4}$), caused by optical fiber material (glass) density fluctuations,
- < 200 nm (0.2μm) absorption in UV region from valence to conduction band,
- far IR absorption for II and III harmonic component (1.38 μm and 0.95 μm) of oscillating vibration for O-H bond in OH^- ion or water molecule,
- far IR absorption for vibrational resonance absorption for both OH^- and Si-O bond in silica (1.23 μm)
- IR absorption for vibrational resonance absorption for Si-O bond (9 μm),
- Absorption of metal ions (Cu^{+2}, Cr^{+2} , Fe^{+2}) admixtures and hydrogen H_2 (1.24 μm),
- Irregularities in optical fiber structure (microbends, diameter fluctuations)

Dispersion and absorption cause that dependency of attenuation of quartz glass correspond to the characteristic presented in Fig. and Table . As we notice, attenuation in visible range is very high, of the order of 30 dB/km. Approaching IR, in the range of 850-860 nm attenuation averages only about 3 dB/km. Around the wavelength 0.95 μm attenuation increases because of absorption for overtone (upper partial) oscillating vibration O-H bond in OH^- ion or water molecule (I water peak). Range of frequencies 850-860 nm is called I optical window. Between I and II water peak (1.38 μm) II optical window with attenuation of order of 0.5-0.3 dB/km is located. Behind the water peak of 1.38 μm III optical window extends with lowest attenuation of the order of 0.2 dB/km. Because of very high signal intensity loss, I optical window in the range 850-860 nm, historically the oldest, is currently applied for distances up to a dozen or so kilometers, e.g. in LAN networks, and is characterized by data flow capacity below Gb/s·km. In I optical window multimode step-index fibers are applied. Despite high attenuation, cheap light sources – electroluminescence diodes, cause the window to be attractive. In II window, which employs radiation of 1310 nm, more expensive fibers are applied – multimode gradient-index and single mode fibers. Because of much lower attenuation signals are transmitted over longer distances, up to 100 km, without regeneration, and transmission itself is faster, up to 80 Gb/s·km. In III optical window we can distinguish two bands: C (1550nm) and L(1625 nm). In this range single mode fibers are used. Thanks to low attenuation signals are transmitted over longer distances, up to 200 km between regenerators, and throughput can reach over 200 Gb/s·km. Together with development in fiber production technology it became possible to overcome attenuation barrier around 1400 nm, caused by OH^- ions absorption. The band used in this range is named E band. Table presents transmission bandwidths currently utilized in multiplexing techniques WDM, and Fig. illustrates the development in minimizing the attenuation in individual spectral regions in 1980s and 1990s.
Table 1.2. Transmission windows utilized in multiplexing techniques WDM.

Window	Wavelength (nm)
I band	850
II band O	1260-1360
V band E	1360-1460
S band	1460-1530
III band C – erb window	1530-1565
IV band L	1565-1625
VI band U	1625-1675

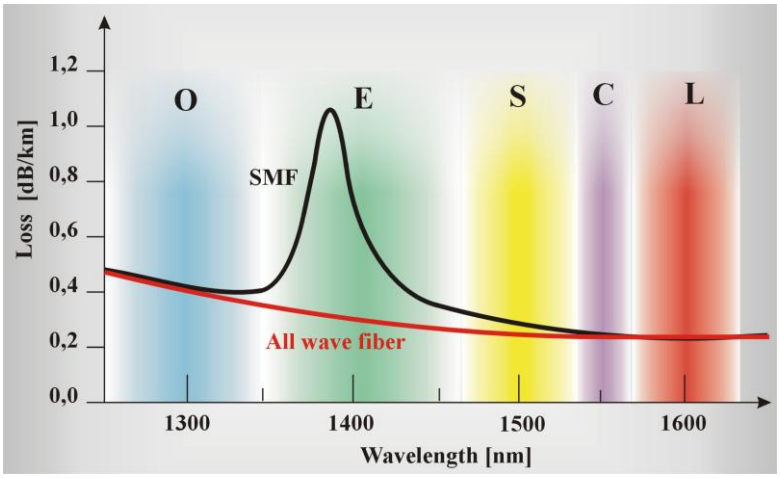

Rys.1.42. Transmission bands utilized in multiplexing techniques WDM.

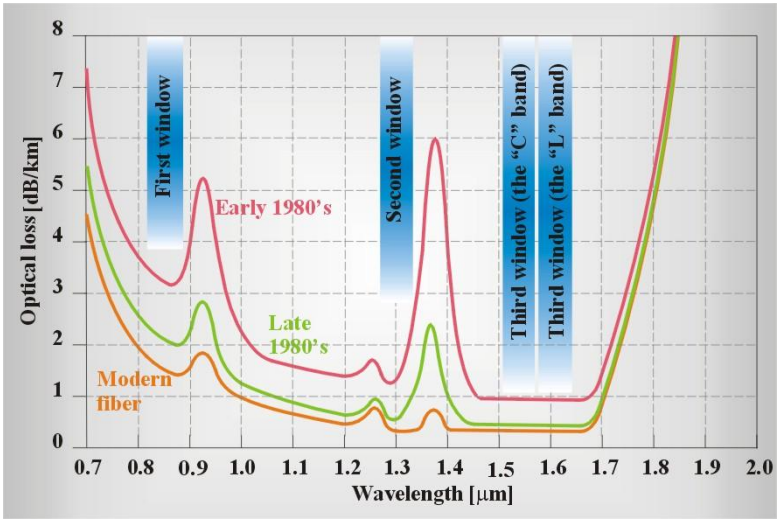

Fig.1.43. Spectral range used nowadays in optical fibers.

1.9. Generations of Optical Fiber Transmission

The history of fiber optics techniques development was presented in numerous monographs [1-6]. Thus here we will only discuss abridgement showing successive phases of fiber optics techniques development. We can distinguish five generations:

First generation – Optical fibers were used were used for the first time by American Army in early 1970s. in order to improve communications. American Navy first installed fiber optics telephone line. Next, in 1976 the Air Force developed their own fiber optics programme, known under the name Airborne Light Optical Fiber Technology (ALOFT). Civilian applications begun in 1977, when both AT&T and GTE installed fiber optics telephone system in Chicago and Boston. The first fiber systems worked in first optical window, 850nm, with optical loss c.a. 4dB/km and throughput below 50Mb/s, utilizing multimode step-index fibers.

Second generation – had been developing since 1987, when most of the companies moved their transmissions to II optical window of 1310 nm and attenuation about 0.5 dB/km with application of single mode fibers with close to zero dispersion.

Third generation – started in 1977 by Nippon Telegraph and Telephone (NTT) by utilizing the transmission in III window, 1550 nm, it developed in 1990s. Transmission in III window is characterizes by low attenuation (from 0.16 to 0.2 dB/km) which greatly increases the range (without regeneration up to 300 km). The main disadvantage is high dispersion (15 – 20 ps/km*nm).

Fourth generation – in IV window close to 1625 nm, is currently being developed. Even though attenuation in IV window is comparable to that of III window, it considerably simplifies introduction of broad-band optical amplifiers EDFA and wavelength division multiplexing WDM.

Fifth generation – is the newest achievement in soliton transmission, which theoretically lead to indefinite increase in transfer capacity. In 1990 Bell Labs sent 2.5 Gb/s signal for the distance of 7500 km without regeneration. The system utilized soliton laser and optical amplifier EDFA. In 1998 the same company sent 100 simultaneous signals, each with the speed 10 Gb/s, using WDM technique over 400 km distance, thus total throughput reached Tb/s (10^{12} bites per second).

Other records in fiber optics transmission development are presented below:

1990-1995 2.5 Gb/s in single fiber, 1 channel, TDM, 80-150 km without regeneration

1997 10 Gb/s in single fiber, 1 channel, TDM

RECORDS in backbone networks DWDM in single fiber:

-September, 2000, Alcatel, 5.12Tb/s

-October, 2000, NEC, 6.4Tb/s on the distance of 186 km

- 2003, Alcatel, 10.1Tb/s on the distance of 300 km and 5.0 Tb/s in the range up to 2000 km

PRACTICAL APPLICATIONS (2003) in backbone networks DWDM in single fiber: 40 Gb/s for single wavelength , 160 channels, 40Gb/s*160=6.4 Tb/s.

Summary

Table 1.3

Optical fiber type	**Characteristics**
MMF - Multi Mode Fiber	850nm, useful on short distances, not applicable in multiplexing technologies WDM, high attenuation about 4dB/km, high dispersion, low throughput below 1Gb/s·km
Standard SMF - Single Mode Fiber	ITU-T G.652 standard recommendation, step refractive index, zero dispersion in II optical window, high dispersion in III optical window 1550 nm, about 17 ps/nm*km, low attenuation and low susceptibility to non-linear effects in III optical window, suitable for single-channel applications in II window and in multi-channel applications in multiplexing technologies DWDM on short distances.
DS- SMF – Dispersion Shifted-Single Mode Fiber,	G.653 standard recommendation, gradient refractive index, strongly negative dispersion in II window (below 20 ps/nm*km) zero dispersion for 1550 nm in III window, application in single-channel transmissions over long distances in III window, little suitability in multi-channel transmission in III window, because lack of dispersion causes cross-talk as the result of four wave mixing FWM.
NZDS- SMF – Non Zero Dispersion Shifted-Single Mode Fiber	G.655 standard recommendation, little but non-zero dispersion in whole optical amplifiers EDFA transfer range (1530-1565 nm) limition non-linear effects of four wave mixing FWM and cross phase modulation CPM, thus far the best medium for DWDM transmissions in III window over long distances.

ITU-T International Telecommunication Union – Telecommunication Standarization Sector

Table.1.4. Non Zero Dispersion Shifted-Single Mode Fiber NZDS- SMF

True Wave	1994, Lucent Technologies, True Wave + and True Wave – variants (alternating dispersion) allowed to achieve without

	regeneration transmission up to about 1000 km with speed 2.5 Gb/s or 300 km z with speed 10 Gb/s
All Wave	Bell Laboratory (Lucent), transmission in all four optical windows II, III, IV, V. Thus far transmission in V window was unavailable because of high attenuation caused by OH^- ions absorption
LEAF	Large Effective Area, 1998, Corning , lower noise, allows to increase the distance between consecutive EDFA amplifiers to over 100 km
TERALIGHT	1999, Alcatel, zero dispersion for 1440 nm, slightly positive dispersion inclination in whole transmission range of EDFA amplifiers, perfect fiber for long distance multi-channel transmissions UWDM

References

1. B. Ziętek, *Optoelektronika*, Wydawnictwo Uniwersytetu Mikołaja Kopernika, 2005
2. G. P. Agrawal, *Nonlinear Fiber Optics*, Academic Press, San Diego, Third Edition, 2001, Chap.2
3. D. Marcuse, *Theory of Dielectric Optical Waveguides*, Academic Press, San Diego,CA, 1991, Chap.2
4. A.W. Snyder, J.D. Love, *Optical Waveguide Theory*, Chapman and Hall, London, 1983, Chaps. 12-15
5. J.A. Buck, *Fundamentals of Optical Fibers*, Wiley, New York, 1995, Chap.3
6. J. Siuzak, *Wstęp do telekomunikacji światłowodowej*, Wydawnictwa Komunikacji I Łączności, Warszawa, 1997, 1999
7. W.van Etten, J.van der Plaats: Fundamentals of Optical Fiber Communications, Prentice Hall, New York 1991
8. D. Marcuse, *Loss analysis of single mode fiber splices*, Bell System Technical Journal, vol.56, no.5, str. 703-718, 1977
9. R.B. Dyott, Elliptical Fiber Waveguides, Artec House, Boston, 1995]
10. R. Feynmann, R. B. Leighton, M. Sands, Feynman's Lectures in Physics, Vol. 2, chapter2

Attachment

Physical quantities in Maxwell equations

Symbol	**Physical quantity**	**SI unit**	**Denotation**
E	Electric field intensity	Volt per meter	V/m
D	Electric induction	Coulomb per square meter	C/m^2
P	Polarization	-	-
H	Magnetic field intensity	Ampere per meter	A/m

M	Magnetization	-	-
j	Current density	Ampere per square meter	A/m^2
B	Magnetic induction	Tesla	T
ρ	Electric charge density	Coulomb per cubic meter	C/m^3
σ	Electric conduction	Siemens per meter	S/m
μ	Magnetic permeability	Henr per meter	H/m
ε	Electric permittivity	Farad per meter	F/m

Symbol	**Physical quantity**	**Value**
c	Light speed in free space	$2.998 \cdot 10^8$ m/s
μ_0	Magnetic permeability of free space	$4p \cdot 10^{-7}$ H/m
ε_0	Electric permittivity of free space	$8.854 \cdot 10^{-12}$ F/m